ShhN-mediated activation of Smo in the absence of Ptch1/2 function

Catalina Casillas and Henk Roelink

Department of Molecular and Cell Biology, 16 Barker Hall, 3204, University of California, Berkeley CA 94720, USA

roelink@berkeley.edu

Abstract

Contrary to the canonical model of Hh signaling, we find that cells genetically lacking *Ptch1* and *Ptch2* remain responsive to ShhN. These cells retain the ability to migrate towards a source of ShhN, while expression of ShhN results in a robust activation of the transcriptional Hh response; both occur in a Smo-dependent manner. This activation of Hh responses does not require binding to the co-receptors Boc, Cdo, or Gas1, nor Shh autocatalytic processing, as the cholesterol moiety on Shh impedes signaling. Shh mutants unable to bind their cognate receptors, or fail to undergo proper processing, nevertheless retain their ability to activate the Hh response both in vivo and in vitro. Together, our findings support a model in which the role of Ptch1/2 as an inhibitor of Smo intersects with a Shh-mediated Smo activation event that is independent of known Shh receptors.

Introduction

Sonic Hedgehog (Shh) is a signaling molecule indispensable for vertebrate embryonic development and adult stem cell niche maintenance (Ingham and McMahon, 2001). Impaired regulation of the Hedgehog (Hh) pathway is a known cause of various birth defects and diseases (Bale, 2002).

In the absence of the Hh ligands, the receptors Patched1 (Ptch1) and Patched2 (Ptch2) inhibit the signal transducer Smoothened (Smo) through a sub-stoichiometric mechanism (Alfaro et al., 2014; Taipale et al., 2002; Zhang et al., 2001a). Ptch1/2 belong to the Resistance, Nodulation, and Division (RND) family of transmembrane transporters, and their inhibition requires the putative proton anti-porter activity that characterizes these molecules (Taipale et al., 2002). In general, RNDs mediate the secretion of small lipophilic and amphipathic molecules (Nikaido and Zgurskaya, 2001; Nikaido and Takatsuka, 2009), and it has been proposed that Ptch1/2 re-localize a sterol that modifies Smo activity (Huang et al., 2016; Taipale et al., 2002).

The binding of extracellular Shh requires Ptch1/2 in conjunction with the co-receptors, Boc, Cdo, and Gas1 (Allen et al., 2011; Izzi et al., 2011; Marigo et al., 1996). Shh is internalized during signaling, causing a change in the subcellular distribution and activity of Smo (Aanstad et al., 2009; Bijlsma et al., 2012; Incardona et al., 2002; 2000; Milenkovic et al., 2009). How these events regulate Smo activity remains unclear. The Hh pathway is upregulated in *Ptch1* null mice and neuralized *Ptch1*$^{LacZ/LacZ}$;*Ptch2*$^{-/-}$ mouse embryonic stem cells, supporting the canonical model that Smo activity is principally regulated by changes in Ptch1/2-mediated inhibition (Alfaro et al., 2014; Goodrich et al., 1997). A tenet of this model is that Smo is constitutively active in the absence of Ptch1/2 function.

Smo is a Class F G-protein coupled receptor (GPCR) and belongs to the superfamily of receptors predominantly defined by Frizzleds (Frz), the canonical receptors of the Wnt signaling pathway (Bhanot et al., 1996; Kristiansen, 2004). Smo and Frzs share over 25% sequence identity and harbor a conserved extracellular, amino-terminal Cysteine Rich Domain (CRD) and seven hydrophobic domains. The CRD of Frz binds to Wnt through two distinct binding sites, one of which is a protein-lipid interface, to initiate signal transduction (Janda et al., 2012). Similarly, the CRD of Smo has been shown to bind to a variety of sterols (Myers et al., 2013; Nachtergaele et al., 2013; Nedelcu et al., 2013), including cholesterol (Huang et al., 2016), which can modulate Smo activity. Smo can also be regulated by small molecule agonists and antagonists that target its membrane-exposed heptahelical domain. This heptahelical domain of Smo is thought to be the target of the inhibitory effect of Ptch1 (Chen et al., 2002a; 2002b; Wang and McMahon, 2013).

Our results support earlier observations that Smo activity can be regulated in a Ptch1/2 independent manner, by demonstrating that ShhN can mediate the activation of Smo in cells lacking Ptch1/2.

Ptch1 and Ptch2 are dispensable for a cell's ability to migrate towards a source of ShhN, a Hh response that nevertheless requires Smo. Although exogenously supplied ShhN does not induce a transcriptional Hh response in cells lacking Ptch1/2, transfection of *ShhN* causes a significant Smo-dependent activation of the transcriptional response. The mechanism regulating cell-autonomous Smo activation is fundamentally different from non-cell autonomous activation via the canonical Shh receptors. Shh mutants unable to bind to canonical Hh receptors, or unable to undergo post-translational processing, retain their ability to induce the Hh response after expression in cells lacking Ptch1/2, as well as after expression in the developing neural tube. Our work reveals a more complex model of Shh signal transduction in which the role of Ptch1 as a catalytic inhibitor of Smo activity intersects with a relatively direct interaction between Shh and Smo, together regulating the definitive level of pathway activation.

Results

The CRD of Smo is not required for its inhibition by Ptch1/2

Sterols have long been proposed to be the cargo which Ptch1 transports across membranes to regulate Smo activity, leaving open the possibility that the CRD of Smo is the target of Ptch1 function. While this issue remains unresolved, it has been shown that a form of Smo lacking its CRD (SmoΔCRD) has reduced sensitivity to Shh signaling (Myers et al., 2013; Nachtergaele et al., 2013) and increased constitutive activity (Byrne et al., 2016). To determine whether Ptch1 targets the CRD of Smo, we used *Ptch1*$^{LacZ/LacZ}$;*Ptch2*$^{-/-}$ fibroblasts derived from mouse embryonic stem cells (mESCs) (Roberts et al., 2016) to assess Ptch1 function in the absence of endogenous Ptch1/2 activity. Transfection of either *Smo* or *SmoΔCRD* into *Ptch1*$^{LacZ/LacZ}$;*Ptch2*$^{-/-}$ cells moderately raised the level of Hh pathway activity (Figure 1A), measured using a well-characterized *Gli-Luciferase* reporter (Taipale et al., 2002). Co-transfection of *Smo* or *SmoΔCRD* together with *Ptch1* or *Ptch1ΔL2* (a dominant inhibitory form of Ptch1 (Briscoe et al., 2001)), predictably lowered Hh pathway activity caused by *Smo* expression. However, co-transfection of *Smo* or *SmoΔCRD* with forms of Ptch1 that contain mutations within the putative antiporter domain, *Ptch1D499A* and *Ptch1ΔL2-D499A*, were less effective at inhibiting the Hh pathway activity caused by *Smo* overexpression (Figure 1A). Thus Smo, including forms lacking its CRD, remains subject to the inhibitory effects of the proton antiporter activity of Ptch1, demonstrating that the CRD of Smo is not the target of Ptch1-mediated inhibition.

80 To verify our observation *in vivo*, we assessed the ability of Ptch1 to inhibit SmoΔCRD in the
81 developing embryo. Electroporation of the chick neural tube is a well-established procedure to
82 introduce transgenes into a normally developing embryo (Itasaki et al., 1999). Electroporation of *Smo*
83 into stage 10-11 (Hamburger and Hamilton, 1951) chick neural tubes did not affect the Hh response
84 pathway (Figure 1B-D). However, electroporation of *SmoΔCRD* resulted in an expansion of the
85 ventral neural markers Nkx2.2 and Mnr2 (Figure1E-G), indicative of an ectopic activation of the Hh
86 response pathway. Intrinsic activation of *SmoΔCRD* has been observed before (Byrne et al., 2016),
87 which indicates that the CRD of Smo is able to regulate its downstream activity. We find that the
88 activity of SmoΔCRD remains subject to Ptch1-mediated inhibition *in vivo* as well, as electroporation
89 of *SmoΔCRD* together with *Ptch1ΔL2*, reversed the phenotypic effects of *SmoΔCRD* expression
90 (Figure 1H-J). SmoΔCRD has been shown to constitutively localize to the primary cilium, the cellular
91 compartment where it mediates the transcriptional Hh response (Aanstad et al., 2009). The entry of
92 Smo into the cilium is required for transcriptional pathway activation, and we find that electroporation
93 of a form of SmoΔCRD that cannot localize to the primary cilium, *SmoΔCRD-CLD* (Aanstad et al.,
94 2009; Corbit et al., 2005), did not result in ectopic activation of the pathway *in vivo* (Figure 1K-M).
95 These results demonstrate that the CRD of Smo is not required for its inhibition by Ptch1, and thus
96 lends support to the idea that the heptahelical domain of Smo is the target for Ptch1 inhibition.

97 SmoΔCRD is intrinsically active *in vivo* (Figure 1E-G), while the activity of Smo and SmoΔCRD in
98 *Ptch1*$^{LacZ/LacZ}$;*Ptch2*$^{-/-}$ cells is indistinguishable (Figure 1A). To evaluate Smo activity in cells lacking
99 all Ptch activity, we derived fibroblasts from *Ptch1*$^{LacZ/LacZ}$;*Ptch2*$^{-/-}$;*Smo*$^{-/-}$ mESCs (Robertson et al.,
100 2016). We assessed the intrinsic activity of Smo and its mutant derivatives in these cells by
101 transfecting the *Gli-Luciferase* reporter with *Smo*, *SmoΔCRD*, *SmoΔCRD-CLD*, *SmoM2* (an
102 intrinsically active mutant (Xie et al., 1998)), *SmoL112D-W113Y* (a mutant unable to bind sterols
103 within the CRD (Nachtergaele et al., 2013)), or *Drosophila Smo*. Remarkably, none of these mutant
104 forms of Smo induced the Hh response better than wild type (Figure 1N). Overall, SmoΔCRD-CLD,
105 SmoL112D-W113Y and Drosophila Smo were less able to induce the transcriptional Hh response
106 compared to Smo, *SmoΔCRD*, and SmoM2 (Figure 1N). This observation is consistent with the
107 notion that SmoM2 is refractory to Ptch1/2 regulation, and suggests that an additional activation
108 event may be required to further induce a Hh response.

109 We next tested whether we could further modulate Smo activity with SAG, an agonist that targets
110 the heptahelical domain, in the absence of Ptch1/2 activity. We measured the Hh response using
111 both the *Gli-Luciferase* reporter and the endogenous *Ptch1:LacZ* reporter contained within *Ptch1*$^{+/LacZ}$
112 and *Ptch1*$^{LacZ/LacZ}$;*Ptch2*$^{-/-}$ fibroblasts. We found that both transcriptional reporters revealed identical
113 results; *Ptch1*$^{LacZ/LacZ}$;*Ptch2*$^{-/-}$ cells were completely insensitive to SAG, a powerful activator of Smo

114 in cells that retain Ptch1/2 activity (Figure 1O). These results indicate that Ptch1/2 function is required
115 for SAG-mediated activation of Smo; and thus might act as an antagonist to the inhibitory activity of
116 Ptch1.

117

118 **ShhN can activate the Hh pathway independent of Ptch1/2 function**

119 As a central ligand in the activation of the Hh response, we assessed whether Shh can affect Smo
120 activity in the absence of Ptch1/2. We have previously demonstrated that Shh-mediated chemotaxis
121 involves the activation of Smo that is quick (in the order of minutes), independent of the primary
122 cilium (Bijlsma et al., 2012), and independent of Ptch1 (Alfaro et al., 2014); leaving open the
123 possibility that Ptch2 serves as the primary receptor. We tested the ability of *Ptch1*$^{LacZ/LacZ}$;*Ptch2*$^{-/-}$
124 fibroblasts to migrate towards a localized source of ShhN (a soluble form of Shh) using a modified
125 Boyden chamber (Chen, 2005). We found that *Ptch1*$^{LacZ/LacZ}$;*Ptch2*$^{-/-}$ cells were indistinguishable from
126 *Ptch1*$^{LacZ/LacZ}$ cells in their ability to migrate towards ShhN (Figure 2A). Shh chemotaxis was largely
127 abolished in *Ptch1*$^{LacZ/LacZ}$;*Ptch2*$^{-/-}$;*Smo*$^{-/-}$ cells, although these cells were retained the ability to
128 migrate towards FCS, our positive control (Figure 2A). These results demonstrate that all Ptch1/2
129 function is dispensable for the activation of Smo by exogenous ShhN. As the Shh co-receptor Boc
130 has been implicated in the Shh-mediated guidance of commissural growth cones towards the floor
131 plate (Okada et al., 2006), we made a fibroblast line that, besides Ptch1/2, also lack Boc, its paralog
132 Cdo, as well as the co-receptor Gas1. We found that *Ptch1*$^{LacZ/LacZ}$;*Ptch2*$^{-/-}$;*Shh*$^{-/-}$;*Boc*$^{-/-}$;*Cdo*$^{-/-}$;*Gas1*$^{-/-}$
133 cells, like all cell lines tested, retain their ability to migrate towards FCS; however, their ability to
134 migrate towards ShhN is impaired, but not completely abolished (Figure 2A).

135 These findings are not readily reconciled with our earlier observation that *Ptch1*$^{LacZ/LacZ}$;*Ptch2*$^{-/-}$ cells
136 cannot upregulate the transcriptional Hh response when exposed to exogenous ShhN, unless
137 transfected with *Ptch1* (Roberts et al., 2016). Since Ptch1 mediates the internalization of Shh during
138 signaling (Incardona et al., 2000), we tested whether we could circumvent this function of Ptch1 by
139 providing ShhN intracellularly through transfection of a *ShhN* construct. Using a panel of cell lines
140 lacking various combinations of *Ptch1* and *Ptch2*, we found that transfection of *ShhN* invariably
141 induced an upregulation of the transcriptional Hh response regardless of the presence or absence
142 of Ptch1/2 (Figure 2B, C). The induction of the Hh response was measured using both a transfected
143 *Gli-Luciferase* reporter (Figure 2B), as well as the genetically encoded *Ptch1:LacZ* reporter
144 (Goodrich et al., 1997) (Figure 2C). The finding that *Ptch1*$^{LacZ/LacZ}$;*Ptch2*$^{-/-}$ cells cannot activate the
145 transcriptional Hh pathway in response to extracellular ShhN indicates that signaling is occurring
146 intracellularly in cells lacking Ptch1/2, and is not the result of non-cell autonomous signaling;

147 henceforth we will refer to this as “cell-autonomous activation”. In all cases, we found that the Smo
148 specific inhibitor Vismodegib (Rudin, 2012) significantly blocked the induction, demonstrating that
149 the transcriptional Hh response caused by *ShhN* transfection is mediated by Smo (Figure 2B, C).
150 We found a high level of cilial occupation by Smo:GFP (Figure 2D) in *Ptch1*$^{LacZ/LacZ}$;*Ptch2*$^{-/-}$ cells,
151 consistent with earlier observations in *Ptch1*$^{-/-}$ cells (Rohatgi et al., 2007). Transfection of *ShhN* in
152 *Ptch1*$^{LacZ/LacZ}$;*Ptch2*$^{-/-}$ cells caused a small, but significant increase in the cilial occupation of
153 Smo::GFP (Figure 2D), a demonstrated output of the transcriptional Hh response. Together these
154 results demonstrate that ShhN can mediate activation of the Hh response pathway via a mechanism
155 that does not require Ptch1/2 function.

156 We found that the *Ptch1*$^{LacZ/LacZ}$ fibroblast cell line has a higher level of intrinsic pathway activity
157 compared to the *Ptch1*$^{LacZ/LacZ}$;*Ptch2*$^{-/-}$ cell line, as measured by both the *Gli-luciferase* and
158 *Ptch1:LacZ* reporters (Figure 2, Figure Supplement 1). Our results that Vismodegib treatment lowers
159 the basal level of pathway activity in *Ptch1*$^{LacZ/LacZ}$ cells is consistent with this observation. However,
160 the induction of transcriptional pathway activity caused by *ShhN* transfection in *Ptch1*$^{LacZ/LacZ}$ cells,
161 as well as the ability of these cells to migrate towards a source ShhN, demonstrate that the absence
162 of Ptch1 does not result in full activation of the Hh response; necessitating additional mechanisms
163 by which Smo can be activated in the absence of Ptch1. The *Ptch1*$^{LacZ/LacZ}$ fibroblast line was derived
164 from mutant embryos, while we derived the compound mutant fibroblast line from embryonic stem
165 cells. The methods by which these cells were derived may explain the differences in their basal level
166 of Hh pathway activity; epigenetically, these cells are expected to be quite different. This notion is
167 supported by the characteristics of a Ptch1 null, Ptch2 containing fibroblast line (*Ptch1*$^{-/-}$;*Disp1*$^{-/-}$;*Shh*$^{-}$
168 $^{/-}$) we derived from mESCs; which, unlike the *Ptch1*$^{LacZ/LacZ}$ line, retains a low level of intrinsic pathway
169 activity similar to the *Ptch1*$^{LacZ/LacZ}$;*Ptch2*$^{-/-}$ cell line, however remains equally sensitive to *ShhN*
170 transfection (Figure 2B).

171 Despite differences in the levels of endogenous Hh pathway activity, we found that co-transfection
172 of *Gli-Luc* with *Ptch1* or *Ptch1ΔL2* effectively inhibited the transcriptional Hh pathway in both
173 *Ptch1*$^{LacZ/LacZ}$ and *Ptch1*$^{LacZ/LacZ}$;*Ptch2*$^{-/-}$ cells (Figure 2, Figure Supplement 2A). Forms of Ptch1
174 lacking the putative antiporter function, Ptch1D499A and Ptch1ΔL2-D499A, were less effective
175 inhibitors of the Hh response pathway than their antiporter-competent counterparts. Transfection of
176 *Gli3*^{PHS}, a dominant inhibitory form of Gli3 (Meyer and Roelink, 2003), efficiently repressed the level
177 of Hh pathway activity in both cells lines (Figure 2, Figure Supplement 2A), while overexpression of
178 *Gli1* caused a significant 10-fold induction (data not shown). These results demonstrate that,
179 regardless of the basal state of the pathway, both cells lines predictably respond to inhibitory
180 elements and thus retain all of the proper components of Hh pathway regulation. To test whether the

181 transcriptional Hh response caused by ShhN transfection is subject to the same regulation, we co-
182 transfected *ShhN* with either *Ptch1ΔL2 or Gli3*^{PHS}. We found that the induction caused by *ShhN*
183 transfection was inhibited by Ptch1ΔL2, demonstrating that ShhN-activated Smo remains subject to
184 Ptch1 inhibition in both *Ptch1*$^{LacZ/LacZ}$ and *Ptch1*$^{LacZ/LacZ}$;*Ptch2*$^{-/-}$ cells (Figure 2, Figure Supplement
185 2B). The relative decrease of Smo activity caused by Ptch1 inhibition is similar under all conditions,
186 which supports the idea that Ptch1 is a non-competitive inhibitor of Smo activation by ShhN.
187 Similarly, *Gli3*^{PHS} was able to repress the induction caused by *ShhN* transfection, implicating the
188 canonical Gli transcription factors as the mediators of this Hh response. These results validate the
189 Gli-Luciferase reporter as a faithful representation of the state of the Hh pathway in these cells.

190

191 **Ptch1/2-independent cell-autonomous activation of the Hh response does not require Boc,**
192 **Cdo or Gas1**

193 Boc, Cdo, and Gas1 have been shown to function in an overlapping manner as obligate Shh co-
194 receptors with Ptch1/2 during non-cell autonomous Hh signaling (Allen et al., 2011; Izzi et al., 2011;
195 Tenzen et al., 2006). The observation that Ptch1 and Ptch2 are dispensable for the activation of Smo
196 after *ShhN* transfection raises the question whether the Shh co-receptors are involved in detecting
197 ShhN in cells independently of Ptch1/2 during cell-autonomous signaling. We addressed the
198 requirement for Boc, Cdo and Gas1 in two complementary ways. 1) We assessed whether Shh
199 mutants unable to bind to the co-receptors could activate the Hh response cell-autonomously, and
200 2) we tested whether cells lacking the co-receptors remained sensitive to *ShhN* transfection.

201 ShhN-E90A, a previously characterized ShhN mutant, cannot bind to either Boc, Cdo, or Gas1, and
202 is unable to activate the Hh response when applied to wildtype cells (Izzi et al., 2011). To
203 independently assess the requirement of Ptch1/2 binding in cell-autonomous pathway activation, we
204 utilized a ShhN mutant with a disrupted zinc coordination site predicted to perturb Ptch1 binding,
205 ShhN-H183A (Fuse et al., 1999; Goetz et al., 2006). We first tested the ability of ShhN-E90A and
206 ShhN-H183A to signal non-cell autonomously (*in trans*), by transfecting *Ptch1* and *Gli-Luc* into
207 *Ptch1*$^{LacZ/LacZ}$;*Ptch2*$^{-/-}$ "reporter" cells and co-culturing them with *Ptch1*$^{LacZ/LacZ}$;*Ptch2*$^{-/-}$ cells
208 independently transfected with *ShhN*, *ShhN-E90A*, or *ShhN-H183A* (Figure 3A, seafoam green). We
209 confirmed our earlier observations that Ptch1-expressing *Ptch1*$^{LacZ/LacZ}$;*Ptch2*$^{-/-}$ reporter cells
210 activated the Hh response when co-cultured with *ShhN* expressing cells (Figure 3C). Reporter cells
211 did not activate the Hh response when cultured with *ShhN-E90A* expressing cells (Figure 3C),
212 corroborating previously published data that ShhN-E90A is unable to mediate Hh signaling *in trans*
213 (Izzi et al., 2011). Consistent with its predicted inability to bind to Ptch1, we find that ShhN-H183A

214 did not activate the Hh response in reporter cells (Figure 3C). These results support previous
215 observations that activation of the transcriptional response by ShhN in the extracellular space (*in*
216 *trans* signaling) requires the binding of Shh to Ptch1/2 in conjunction with the co-receptors.

217 ShhN is a widely used mutant form of Shh, it is freely soluble while retaining its inductive properties
218 (Bumcrot et al., 1995a; Roelink et al., 1995). A significant distinction between ShhN and fully matured
219 Shh is that Shh has a cholesterol moiety that serves as a membrane anchor (Yang et al., 1997). The
220 distinct differences in distribution and extracellular transport between cholesterol-modified and
221 soluble forms of Shh might have significant ramifications for their activities. This led us to test the
222 ability of Shh and mutant derivatives expected to be cholesterol-modified (ShhE90A and ShhH183A)
223 to signal *in trans*. *Ptch1*$^{LacZ/LacZ}$;*Ptch2*$^{-/-}$ reporter cells (transfected with *Gli-Luc* and *Ptch1*) activated
224 the Hh response pathway when co-cultured with Shh and ShhE90A expressing cells, but not with
225 ShhH183A expressing cells (Figure 3E). This result indicates that the cholesterol modification of Shh
226 is able to compensate for the inability to bind Cdo, Boc or Gas1 when signaling *in trans*. The inability
227 of ShhH183A to signal *in trans* may be due, in part, to its poor autocatalytic cleavage, which is directly
228 linked to its modification with a cholesterol moiety (Figure 3B) (Goetz et al., 2006).

229 We assessed the role of co-receptor binding during cell-autonomous Hh signaling by transfecting
230 mutant forms of *ShhN*, *ShhN-E90A* and *ShhN-H183*, into *Ptch1*$^{LacZ/LacZ}$;*Ptch2*$^{-/-}$ cells together with the
231 *Gli-Luc* reporter (Figure 3A, lilac). We found that, similar ShhN, both ShhN-E90A and ShhN-H183A
232 significantly activated the Hh pathway in *Ptch1*$^{LacZ/LacZ}$;*Ptch2*$^{-/-}$ cells (Figure 3D); indicating that neither
233 Boc, Cdo, nor Gas1 are required for cell-autonomous pathway activation. We next evaluated whether
234 the cholesterol modification on Shh mutants affects cell-autonomous pathway activation by
235 transfecting *Shh* constructs together with the *Gli-Luc* reporter in *Ptch1*$^{LacZ/LacZ}$;*Ptch2*$^{-/-}$ cells (Figure
236 3A, lilac). We found that transfection of *Shh* into *Ptch1*$^{LacZ/LacZ}$;*Ptch2*$^{-/-}$ cells results in a minute
237 increase of pathway activity (Figure 3F), suggesting that the cholesterol modification on Shh is a
238 major impediment to cell-autonomous activation of the Hh response. In contrast, transfection of
239 *ShhE90A* or *ShhH183A* resulted in a significantly greater pathway induction (Figure 3F). The poor
240 autoproteolysis observed with ShhH183A, which would prevent its cholesterol modification, makes
241 this result difficult to interpret; however, all together these results suggest that Shh interaction with
242 Boc, Cdo or Gas1 impedes cell-autonomous Hh signaling with cholesterol-modified Shh. We
243 confirmed that transfection of these Shh mutants activates a cell-autonomous Hh response in
244 *Ptch1*$^{LacZ/LacZ}$ in a manner similar to *Ptch1*$^{LacZ/LacZ}$;*Ptch2*$^{-/-}$ cells (Figure 3, Figure Supplement 1); again
245 we found that wildtype Shh is a poor inducer of cell-autonomous pathway activation compared to its
246 mutant counterparts.

247 To further verify the observation that Boc, Cdo and Gas1 are not a required component of the cell-
248 autonomous Hh response, we generated a *Ptch1*$^{LacZ/LacZ}$;*Ptch2*$^{-/-}$;*Boc*$^{-/-}$;*Cdo*$^{-/-}$;*Gas1*$^{-/-}$;*Shh*$^{-/-}$ mESC
249 line and a derived fibroblast line of the same genotype. Upon differentiation into neuralized embryoid
250 bodies, these cells behave similarly to their parental *Ptch1*$^{LacZ/LacZ}$;*Ptch2*$^{-/-}$;*Shh*$^{-/-}$ line (Roberts et al.,
251 2016), and express ventral neural markers indicative of an activated Hh response (Figure 3G). The
252 neural phenotype of differentiated *Ptch1*$^{LacZ/LacZ}$;*Ptch2*$^{-/-}$;*Boc*$^{-/-}$;*Cdo*$^{-/-}$;*Gas1*$^{-/-}$;*Shh*$^{-/-}$ mESCs
253 demonstrates that pathway activation in these cells does not require expression of Shh or the Shh
254 (co-)receptors. Transfection of *ShhN* or any other *Shh* mutant into *Ptch1*$^{LacZ/LacZ}$;*Ptch2*$^{-/-}$;*Boc*$^{-/-}$;*Cdo*$^{-/-}$
255 ;*Gas1*$^{-/-}$;*Shh*$^{-/-}$ fibroblasts cells induced a significant increase of the Hh response (Figure 3H). The
256 independently derived *Ptch1*$^{LacZ/LacZ}$;*Ptch2*$^{-/-}$;*Boc*$^{-/-}$;*Cdo*$^{-/-}$;*Gas1*$^{-/-}$;*Shh*$^{-/-}$ and *Ptch1*$^{LacZ/LacZ}$;*Ptch2*$^{-/-}$
257 fibroblasts behave nearly indistinguishably in this assay.

258 To assess whether cell-autonomous pathway activation is a phenomenon that occurs across all Hh
259 paralogs, we tested the ability of Indian Hedgehog (Ihh) and Desert Hedgehog (Dhh) to activate the
260 Hh pathway after transfection. The soluble forms IhhN and DhhN are similar to ShhN in their ability
261 to induce the Hh response cell-autonomously, whereas wildtype Ihh and Dhh are significantly more
262 potent than Shh (Figure 3I). These findings demonstrate that cell-autonomous pathway activation is
263 a characteristic of all vertebrate Hedgehog paralogs.

264 Together our data confirms that the extracellular receptors Boc, Cdo, and Gas1 are not required for
265 pathway activation mediated by *ShhN* expression in Ptch1/2 null cells. As we found before in
266 *Ptch1*$^{LacZ/LacZ}$;*Ptch2*$^{-/-}$ cells (Figure 3F), expression of wild type Shh in *Ptch1*$^{LacZ/LacZ}$;*Ptch2*$^{-/-}$;*Boc*$^{-/-}$;*Cdo*$^{-}$
267 $^{/-}$;*Gas1*$^{-/-}$;*Shh*$^{-/-}$ only marginally induces the Hh pathway, a further demonstration that the cholesterol
268 moiety prevents cell autonomous signaling by Shh (Figure 3I). This result demonstrates that it is not
269 Boc/Cdo/Gas1 binding that impedes cell-autonomous activation by cholesterol-modified Shh; further
270 analysis is required to understand the activity of ShhE90A

271

272 **Shh mutants unable to bind to canonical receptors induce the Hh response in the developing**
273 **neural tube**

274 Both Ptch1 and Ptch2, as well as Boc, Cdo, and Gas1 have been shown to play central roles in
275 regulation of the Hh responses *in vivo* (Allen et al., 2011; Goodrich et al., 1997; Izzi et al., 2011). We
276 assessed whether expression of Shh mutants can activate the Hh response independent of (co)-
277 receptor interaction in the developing neural tube of chicken embryos. We electroporated stage 10-
278 11 (Hamburger and Hamilton, 1951) chick neural tubes with *ShhN*, *ShhN-E90A*, or *ShhN-H183*
279 together with *GFP*. We found that all ShhN mutants are able to activate the Hh pathway as assessed

280 by changes in Shh-mediated dorsal-ventral patterning (Figure 4A-J). Expression of ShhN, ShhN-
281 E90A, and ShhN-H183A causes extensive dorsal expansion of the Nkx2.2 and Mnr2 domains
282 (Figure 4A-F), as well as repression of Pax7 (Figure 4G-J). These results support our finding that
283 binding to the canonical (co)-receptors is not a necessary component for activation of the Hh
284 response *in vivo*.

285 In order to assess more biologically relevant forms of Shh, we electroporated *Shh*, *ShhE90A,* or
286 *ShhH183A* together with *GFP* in developing chick neural tubes. Expression of *Shh* or *ShhE90A*
287 caused an expansion of Nkx2.2 and Mnr2 domains, as well as a repression of Pax7 (Figure 5A, B,
288 E, F, I, J), indicating that these forms of Shh are active. However, electroporation of *ShhH183A* does
289 not result in extensive activation of the pathway (Figure 5C, G, K). It is unclear why ShhH183A is
290 able to activate the pathway *in vitro* but not *in vivo*. One possibility is that the inability of ShhH183A
291 to efficiently undergo autoproteolysis may prevent pathway activation *in vivo*. To test this hypothesis,
292 we assessed ShhC199A, a form of Shh that is unable to undergo autoproteolytic cleavage (Figure
293 2B) and is unable to mediate signaling *in trans* (Roelink et al., 1995). Electroporation of *ShhC199A*
294 causes an expansion of ventral markers as well as a repression of Pax7 (Figure 5D, H, L). This
295 unanticipated result rejects the hypothesis that the inability of ShhH183A to undergo autoproteolysis
296 is the reason why it is inactive *in vivo*, and this issue remains unresolved. However, the ability of
297 ShhN-E90A, ShhN-183A, and ShhE90A to induce the Hh response in the developing neural tube
298 provides *in vivo* support of our finding that Smo can be activated by ShhN without the need to bind
299 to its canonical (co-)receptors.

300 We stained electroporated neural tubes with the anti-Shh monoclonal antibody 5E1 (Ericson et al.,
301 1996). 5E1 staining pattern on the (left) side of neural tubes overexpressing *ShhN* or *Shh* coincide
302 with *GFP* expressing cells (Figure 3K and 4M). The 5E1 staining of neural tubes expressing ShhN-
303 E90A and in particular ShhE90A is more profuse than neural tubes expressing ShhN or Shh (Figure
304 4L and 5N). There are two plausible explanations for this observation. 1) The inability of Shh to bind
305 to the co-receptors could greater access to the 5E1 epitope, or 2) inactivation of the putative
306 cannibalistic protease activity of Shh (Rebollido-Rios et al., 2014) might result in higher steady state
307 levels of ShhE90A. The 5E1 staining pattern on neural tubes expressing ShhN-H183A, ShhH183A
308 and Shh-C199A reveals only endogenous Shh expression in the floor plate (Figure 4M, 5O, and 5P).
309 The discrepancy between the effects on patterning and the absence of 5E1 staining of these mutants
310 is possibly caused by poor recognition of the uncleaved ligand, in combination with the disruption of
311 the epitope in the H183Shh mutant. Importantly, the lack of ectopic 5E1 staining in embryos
312 expressing ShhN-H183A and ShhC199A that show ectopic activation of the Hh response,

313 demonstrates that the effect on neural tube patterning is mediated by these Shh mutants as such,
314 and not due to secondary induction of endogenous Shh expression.

315

316 **The cell-autonomous activity of ShhN is unaffected by alternate C-terminal extensions, but is**
317 **impeded by the cholesterol modification**

318 The observation that the expression of ShhN, which lacks the C-terminal cholesterol modification, is
319 a much more potent activator of the Hh response than Shh led us to assess the extent to which forms
320 of Shh with varying lipophilic and C-terminal modifications can signal cell-autonomously and *in trans*.
321 We evaluated fully modified Shh, as well as forms of Shh lacking either the cholesterol moiety
322 (ShhN), the palmitoyl moiety (ShhC25S), or both (ShhN-C25S) (Bumcrot et al., 1995b; Gao et al.,
323 2011; Pepinsky et al., 1998; Porter et al., 1996) (Figure 5A).

324 The ability of Shh to signal to *Ptch1*$^{LacZ/LacZ}$;*Ptch2*$^{-/-}$ reporter cells *in trans* (Figure 5A, top diagram)
325 was unaffected by the absence or presence of its lipophilic modifications, with the exception of ShhN-
326 C25S (Figure 5B). The absence of palmitoylation on ShhN results in an inability to signal *in trans*, as
327 observed before (Chen et al., 2004). ShhN with distinct C-terminal extensions have been shown to
328 be active in embryos before: ShhN::CD4 induces digit duplications when expressed in limb buds
329 (Yang et al., 1997), and ShhN::GFP can partially rescue the genetic loss of *Shh* (Chamberlain et al.,
330 2008). Both ShhN::CD4 and ShhN::GFP are membrane bound; ShhN::CD4 by its transmembrane
331 domain in CD4, and ShhN::GFP due a cholesterol moiety at the carboxyterminal end of GFP. Both
332 ShhN::CD4 and ShhN::GFP retain the ability to activate the Hh response *in trans* (Figure 5B).
333 Consistent with previous observations (Roelink et al., 1995), we find that ShhC199A, which is unable
334 to undergo autoproteolytic cleavage, is unable to significantly induce Hh response *in trans*.

335 The finding that cells expressing wild type *Shh* are poorly responsive to their own signal has been
336 reported before (García-Zaragoza et al., 2012), and consistent with the finding that Shh primarily
337 signals *in trans* (Bailey et al., 2009; Tian et al., 2009). This is in stark contrast to the observation that
338 ShhN is a potent cell-autonomous activator. To evaluate the extent to which the lipophilic
339 modifications of Shh affect its ability to activate the Hh response cell-autonomously, we transfected
340 *Ptch1*$^{LacZ/LacZ}$;*Ptch2*$^{-/-}$ reporter cells with constructs coding for various forms of lipid-modified Shh
341 (Figure 5A, bottom diagram). We find that the palmitoylation of Shh has little effect on its poor ability
342 to induce a cell-autonomous response, unlike its activity *in trans* (Figure 5C). Similarly, preventing
343 palmitoylation of ShhN (ShhN-C25S) does not affect its ability to induce the Hh response cell-
344 autonomously. Interaction between the palmitate of Shh and Ptch1 has shown to be critical for
345 repressing Ptch1-mediated inhibition (Tukachinsky et al., 2016), and thus the ability of ShhN-C25S

346 to activate the pathway supports the idea that cell-autonomous pathway activation occurs
347 independently of Ptch1/2-mediated inhibition of Smo. This result is further reinforced by the
348 observation that expression of ShhN-C25S causes an upregulation of the Hh response in the
349 developing neural tube (Figure 6, Figure Supplement 1).

350 The presence of cholesterol on Shh significantly decreases its ability to induce the Hh response cell-
351 autonomously (Figure 6C, 3F, 3I). This decrease in activity is not due to its membrane association,
352 as Shh::CD4 and Shh::GFP are potent cell-autonomous activators of the Hh pathway (Figure 6C).
353 Consistent with the observation that forms of Shh with extraneous C termini are able to induce the
354 Hh response cell-autonomously, we found that the uncleaved ShhC199A mutant also retains the
355 ability to cell-autonomously activate the pathway in *Ptch1*$^{LacZ/LacZ}$;*Ptch2*$^{-/-}$ cells (Figure 6C). These
356 results concur with our observation that ShhC199A can induce the Hh response *in vivo* (Figure 5D,
357 H, L). It appears that an important function of the cholesterol moiety on Shh is to prevent Shh-
358 expressing cells from strongly upregulating the Hh response cell-autonomously. To test whether the
359 cholesterol modification on Shh alters its cellular distribution, we used the 5E1 antibody to stain
360 transfected *Ptch1*$^{LacZ/LacZ}$;*Ptch2*$^{-/-}$ cells for either wildtype Shh or ShhN. We find that Shh is
361 stereotypically localized to the cell membrane, including filopodial extensions (Figure 6D). ShhN is
362 consistently absent from the cell membrane and filopodial structures, and instead occupies a
363 perinuclear location (Figure 6E). This suggests that the processing and subsequent cholesterol
364 modification of Shh regulates its localization within expressing cells, possibly preventing co-
365 localization with Smo or interaction with other proteins. The cholesterol modification biases against
366 the activation of the Hh response in cells that produce Shh, thereby restricting its effects to non-cell
367 autonomous activation of the Hh pathway. Together these results support our observation that many
368 forms of Shh can activate Smo via a mechanism that does not involve any of the known co-receptors.

369

370 **Discussion**

371 The canonical model of Smo activation mediated by the Shh-induced release of Ptch1 inhibition is
372 challenged by our observations. Despite the ample evidence that Ptch1 is an efficient inhibitor of
373 Smo (Goodrich et al., 1997), we find that the loss of *Ptch1/2* does not inevitably result in maximal
374 Smo activation, and that a variety of Shh mutants can activate the migrational and transcriptional Hh
375 responses in the absence of Ptch1/2 function.

376 Whether cells lacking Ptch1 or Ptch2 retain sensitivity to Shh *in vivo* is unclear, however some
377 provocative evidence indicates that they might. The spectrum of tumors observed in *Ptch1* null and

378 in *Ptch1/2* heterozygous mice (Lee et al., 2006), from basal cell carcinomas to medulloblastomas
379 (Goodrich et al., 1997; Lee et al., 2006; Mao et al., 2006), are commonly found at sites where Shh
380 is expressed; and Shh-induced tumors often arise at the same locations (Beachy et al., 2004).
381 According to the canonical model, the loss of Ptch1/2 function should result in the cell-autonomous
382 activation of the Hh response. The positional overlap between tumors induced by the loss of Ptch
383 function and Shh-induced tumors is compatible with our model that cells lacking Ptch1/2 function
384 nevertheless retain some ability to respond to Shh. Our model is further supported by the observation
385 that Smo is required for the establishment of left/right symmetry in mouse embryos, whereas *Ptch1*
386 is not (Zhang et al., 2001b). *Pitx2* expression can be induced by Shh (Ryan et al., 1998), and requires
387 *Smo* as well as *Shh* and *Ihh* (Zhang et al., 2001b). Interestingly, *Ptch1*$^{-/-}$ mutant embryos normally
388 establish asymmetric expression of *Pitx2*, demonstrating that this Hh/Smo-mediated symmetry-
389 breaking event can occur independently of Ptch1. Analysis of *Ptch1*$^{-/-}$;*Ptch2*$^{-/-}$;*Shh*$^{-/-}$;*Ihh*$^{-/-}$ compound
390 null embryos would help to resolve the issue as to what extent the loss of Ptch1/2 activity is epistatic
391 to the loss of Shh and Ihh.

392 In *Drosophila* embryos, the genetic loss of *Ptch* is epistatic to the loss of *Hh* (Bejsovec and
393 Wieschaus, 1993), suggesting that Ptch-independent regulation of Smo does not play a major role
394 during *Drosophila* development. The incongruity between our data and *Drosophila* genetics may be
395 explained by auxiliary molecules involved in *Drosophila* Smo activation that are present in cells
396 lacking Ptch, creating the impression that loss of Ptch-mediated inhibition unequivocally results in
397 Smo activation. However, our model is consistent with the finding that cells in the posterior
398 compartment of the wing imaginal disc retain responsiveness to the Hh ligand independent of Ptch
399 function (Ramirez-Weber et al., 2000), highlighting a mechanism of Smo activation in *Drosophila*
400 akin to the one we observe in *Ptch1*$^{LacZ/LacZ}$;*Ptch2*$^{-/-}$ cells. It is not terribly surprising that Smo,
401 expressed from a single gene in most vertebrates and invertebrates, would have a complex
402 mechanism of regulation and activation, given that it is responsible for relaying most known Hh
403 responses in the organism.

404 Our results demonstrate that a wide variety of Shh mutants, many previously characterized as “dead”
405 signals, retain their ability to activate Smo in cell lines lacking the canonical receptors as well as in
406 wildtype cells within developing embryos. Of all the forms of Shh tested, wildtype Shh is unique in
407 that it is unable to induce the cell-autonomous Hh response, while it can still efficiently signal non-
408 cell autonomously. In stark contrast, ShhC199A, which remains unprocessed as a full length
409 precursor, cannot signal to neighboring cells, but is an efficient inducer of the Hh response cell-
410 autonomously. These results indicate that an important function of the unusual processing and
411 modification of Shh is to prevent activation of the Hh response in cells that express the ligand, thus

412 reinforcing strict non-cell autonomous signaling. The ability of ShhC199A to induce the Hh response
413 autonomously came as a surprise, and this switch between cell-autonomous to non-cell autonomous
414 activity upon cleavage has implications for the understanding of diseases associated with mutations
415 in *Shh*.

416 Several *Shh* mutations that cause Holoprosencephaly result in forms of Shh that fail to
417 autoproteolytically cleave, which strongly correlates with their inability to induce the Hh response *in*
418 *trans* (Singh et al., 2009; Traiffort et al., 2004). Moreover, many of the otherwise uncharacterized
419 *SHH* mutants found in patients with Holoprosencephaly are located in the C-terminal domain, and
420 thus possibly affect autoproteolytic cleavage (Roessler et al., 2009). We found that ShhC199A is
421 perfectly capable of inducing the Hh response when expressed in the developing neural tube. It
422 appears that many mutations in the C-terminal domain of SHH could give rise to forms that gain the
423 ability to induce the Hh response cell-autonomously. Heterozygous mutations in the C-terminal
424 domain of *SHH* can cause holoprosencephaly (Hehr et al., 2010); however, mice heterozygous for
425 a null *Shh* allele are normal. Two identified *Shh* mutations that cause Holoprosencephaly change
426 the Cysteine residue at position 198 that is required for Shh processing (homologous to the C199
427 residue in mice), thus resulting in an obligatory full-length form of Shh (Roessler et al., 2009). Thus,
428 either unprocessed Shh functions as a dominant negative form of Shh, or cell-autonomous activation
429 of the Hh response in cells heterozygous for this mutation contributes to holoprosencephaly. Given
430 our observation that ShhC199A is a potent inducer of the Hh response *in vivo*, we favor the latter
431 explanation.

432 The data we present here, along with recently published results from our lab (Roberts et al., 2016)
433 and data from the literature, supports a model in which Ptch1/2 mediates the allosteric inhibition of
434 Smo by means of its antiporter function in the absence of the Shh ligand. Upon the availability of
435 Shh in the extracellular space, Shh can bind to a receptor complex via the ligand-binding domain
436 (L2) of Ptch1/2. We hypothesize that this event represses the allosteric inhibition mediated by
437 Ptch1/2 (Figure 7). The Shh ligand is internalized by the receptor complex, resulting in its co-
438 localization with Smo in an endocytic compartment where it mediates an orthosteric activation of
439 (disinhibited) Smo. It is important to stress that Shh-mediated activation may not occur through direct
440 binding to Smo. Although Smo was initially considered to be the putative receptor for Hh when it was
441 identified in *Drosophila*, there has been no evidence to support direct binding between Shh and Smo.
442 Many questions about cell-autonomous Hh activation by Shh are left to be explored, however a
443 central question remains: What is the basis of the interaction between Shh and Smo? A
444 multidisciplinary approach of biochemistry, genetics, and bioinformatics may be required to solve
445 this enduring puzzle.

446

447 ## Materials and Methods

448 **Materials:** Vismodegib was a gift from Dr. Fred de Sauvage (Genentech). SAG was from EMD
449 Biochemicals. Recombinant ShhN protein was from R&D Systems. Cell Tracker Green CMFDA was
450 from Invitrogen.

451 **Electroporations:** Hamburger-Hamilton (HH) stage 10 Gallus gallus embryos were electroporated
452 caudally in the developing neural tube using standard procedures (Meyer and Roelink, 2003).
453 Embryos were incubated for another 48 h following electroporation, dissected, fixed in 4% PFA,
454 mounted in Tissue-Tek OCT Compound (Sakura) and sectioned.

455 **Embryoid Body differentiation:** mESCs were neuralized and differentiated into embryoid bodies
456 (NEBs) using established procedures (Wichterle et al., 2002). NEBs were harvested after 5 days in
457 culture, fixed, and stained for Nkx2.2 and Olig2 (Kawakami et al., 1997). NEBs were mounted in
458 Fluoromount-G (Southern Biotech) and imaged.

459 **Immunofluorescence:** Antibodies for mouse Pax7 (1:10), Mnr2 (1:100), Nkx2.2 (1:10), Shh (5E1,
460 1:20) were from the Developmental Studies Hybridoma Bank. The Rabbit α-GFP (1:1000) antibody
461 was from Invitrogen, and the Goat α-hOlig2 (1:100) antibody was from R&D Systems. The mouse
462 α-acetylated tubulin (1:200) was from Sigma Aldrich. Alexa488 and Alexa568 secondary antibodies
463 (1:1000) were from Invitrogen. Nuclei were stained with DAPI (Invitrogen).

464 **DNA Constructs:** The *Gli-Luciferase* reporter and the Renilla control were gifts from Dr. H. Sasaki
465 (Sasaki et al., 1997). *Ptch1* was a gift from Dr. Scott (Stanford University, CA, USA). *Ptch1-Δloop2*
466 was a gift from Dr. Thomas Jessell (Columbia University, NY, USA). *Ptch1* channel mutants were
467 previously described (Alfaro et al., 2014). SmoΔCRD was a gift from J. Reiter (Aanstad et. al., 2009).
468 SmoM2 was from Genentech (F. de Sauvage). The following mutations were created using
469 Quikchange mutagenesis (Stratagene): *Shh-E90A*, *Shh-H183A*, *ShhN-E90A*, *ShhN-H183A*,
470 *SmoΔCRD-CLD*, *SmoL112DW113Y. Shh::GFP* and *Shh::CD4* were gifts from Dr. Andrew McMahon
471 (University of Southern California, CA, USA). Dhh and Ihh were gifts from Charles Emerson Jr.
472 (University of Massachusetts Medical School, MA, USA). *DhhN* and *IhhN* were made by site directed
473 mutagenesis of C199 (Dhh) and C203 (Ihh) to a stop codon. ShhC199A was previously described
474 (Roelink et al., 1995). $Gli3^{PHS}$ was previously described (Meyer et. al., 2003).

475 **Genome Editing:** TALEN constructs targeting the first exon of mouse Cdo and Gas1 were designed
476 and cloned into the pCTIG expression vectors containing IRES puromycin and IRES hygromycin
477 selectable markers (Cermak et al., 2011). The following repeat variable domain sequences were

478 generated: Cdo, 5' TALEN: NN HD NI NG HD HD NI NN NI HD HD NG HD NN NN ; 3' TALEN: HD
479 NI HD NI NI NN NI NI HD NI NG NI HD NI NN; Gas1, 5' TALEN: NN NI NN NN NI HD NN HD HD
480 HD NI NG NN HD HD; 3' TALEN: NN NN NI NI NI NI NN NG NG NG NN NG HD HD NN NI. Two
481 CRISPR constructs targeting a double strand break flanking the first exon of mouse Boc were cloned
482 into pSpCas9 vector with an IRES puromycin selectable marker (Ran et al., 2013). The Boc
483 CRISPRs targeted the following forward genomic sequences (PAM sequences underlined):
484 Upstream of first exon 5' CCTGTCCTCGCTGTTGGTCCCTA 3'; Downstream of first exon 5'
485 CCCACAGACTCGCTGAAGAGCTC 3'. *Ptch1*$^{LacZ/LacZ}$;*Ptch2*$^{-/-}$;*Shh*$^{-/-}$ mouse embryonic stem cells
486 (Roberts et al., 2016) were plated at a density of 1.0x106 on 6-well plates and transfected with 6
487 genome editing plasmids the following day. One day after transfection, selective ES medium (100
488 µg/mL hygromycin and 0.5 µg/mL puromycin) was added for 4 days. Selective medium was removed
489 and surviving mESC colonies were isolated, expanded and genotyped by sequence PCR products
490 spanning TALEN and CRISPR-binding sites.

491 **Genotyping:** PCR screening was performed on cell lysates using primers flanking the TALEN or
492 CRISPR binding sites for the *Boc*, *Cdo*, and *Gas1* loci. *Boc*, (5')
493 CATCTAACAGCGTTGTCCAACAATG and (3') CAAGGTGGTATTGTCCGGATC; *Cdo*, (5')
494 CACTTCAGTGTGATCTCCAG and (3') CCTTGAACTCACAGAGATTCG; Gas1, (5')
495 ATGCCAGAGCTGCGAAGTGCTA and (3') AGCGCCTGCCAGCAGATGAG. PCR products were
496 sequenced. Samples with signals indicative of INDEL mutations were cloned into the pCR-BluntII
497 vector using the Zero Blunt TOPO PCR cloning kit (Invitrogen) and sequenced to confirm allele
498 sequences. A *Ptch1*$^{LacZ/LacZ}$;*Ptch2*$^{-/-}$;*Boc*$^{-/-}$;*Cdo*$^{-/-}$;*Gas1*$^{-/-}$;*Shh*$^{-/-}$ mESC clone was identified harboring a
499 50 bp deletion in Cdo exon 1, a heteroallelic 480 bp insertion and a 200 bp deletion in Gas1 exon1
500 resulting in a premature stop codon in the reading frame, and a 450 bp deletion of Boc exon 1.

501 **Cell Culture:** *Ptch1*$^{LacZ/LacZ}$;*Ptch2*$^{-/-}$, *Ptch1*$^{LacZ/LacZ}$;*Ptch2*$^{-/-}$;*Smo*$^{-/-}$, *Ptch1*$^{-/-}$;*Disp1*$^{-/-}$;*Shh*$^{-/-}$, and
502 *Ptch1*$^{LacZ/LacZ}$;*Ptch2*$^{-/-}$;*Boc*$^{-/-}$;*Cdo*$^{-/-}$;*Gas1*$^{-/-}$;*Shh*$^{-/-}$ fibroblasts were obtained by plating mESCs at a
503 density of 8.0x10^{5} cells in 6-well plates and transfected with the *large T antigen* from the SV40 virus
504 (Gökhan et al., 1998) in ES medium. Cells were then switched to DMEM (Invitrogen) supplemented
505 with 10% fetal bovine serum (FBS) without LIF. *Ptch1*$^{+/LacZ}$ and *Ptch1*$^{LacZ/LacZ}$ fibroblasts (gifts from
506 Dr. Scott) were cultured in DMEM supplemented with 10% FBS (Invitrogen) and maintained under
507 standard conditions. Identity of these lines was confirmed by the presence of the LacZ recombination
508 in the Ptch1 locus, the presence of 40 chromosomes per cell, and mouse-specific DNA sequences
509 of the edited genes. mESC lines were maintained using standard conditions in dishes coated with
510 gelatin, without feeder cells. Cells were routinely tested for Mycoplasm by Hoechst stain, and grown
511 in the presence of tetracycline and gentamycin at regular intervals. Cultures with visible Mycoplasma

512 infection were discarded. None of the cell lines used in this study is listed in the Database of Cross-
513 Contaminated or Misidentified Cell Lines. Fibroblast-like lines derived from the mESCs were re-
514 sequenced at the edited loci to confirm their identity.

515 **Transfection:** Cells were transiently transfected for 24h at 80-90% confluency using Lipofectamine
516 2000 reagent (Invitrogen) according to the manufacturer's protocol.

517 **Modified Boyden Chamber Migration Assay:** Cell migration assays were performed as previously
518 described (Bijlsma et. al. 2007). Cells were labeled with 10 μM CellTracker Green (Invitrogen) in
519 DMEM for one hour. The well compartments were set up with the specified chemoattractant (ShhN
520 .75 μg/ML (resuspended in 0.1%BSA in PBS), 10% FCS, or no attractant (plus 0.1%BSA in PBS)
521 and pre-warmed at 37˚C. Cells were then detached with 5mM EDTA and resuspended in DMEM
522 without phenol red and supplemented with 50mM HEPES. Cells were transferred into FluoroBlok
523 Transwell inserts (BD Falcon) at $5.0x10^4$ cells per insert. GFP-spectrum fluorescence in the bottom
524 compartment was measured every 2 min for 99 cycles (approximately 3 hours), after which
525 background fluorescence (medium without cells) and a no-attractant control was subtracted from
526 each time point. Starting points of migration were set to 0.

527 **Gli-Luciferase Assay:** Fibroblasts were plated at a density of $3x10^4$ in 24 well plates and transfected
528 with *Gli-Luciferase*, *CMV-Renilla* (control plasmid), and specified plasmids 24 hours after plating.
529 Cells were grown to confluency and then switched to low serum medium (0.5% FBS) alone or with
530 specified concentrations of Vismodegib or SAG. After 24 hours, cells were lysed and the luciferase
531 activity in lysates was measured using the Dual Luciferase Reporter Assay System (Promega). Raw
532 Luciferase values were normalized against Renilla values for each biological replicate to control
533 against variation in transfection efficiency. Individual luciferase/renilla values were then normalized
534 against the mock control average for each experiment.

535 **LacZ Assay:** Fibroblasts were plated at a density of $3x10^4$ in 24 well plates and transfected with
536 plasmids 24 hours after plating (or remained untransfected for SAG experiments). Fibroblasts were
537 grown to confluency and then switched to a low serum medium (0.5% FBS) alone or with specified
538 concentrations of Vismodegib or SAG. After 24 hours, cells were lysed and lysates were analyzed
539 using the Galacto-Light™ chemiluminescence kit (Applied Biosciences) for level of LacZ expression.
540 Raw chemiluminescence values were normalized against total protein for each biological replicate.
541 Protein concentration was determined with a Bradford assay using the Bio-Rad Protein Assay Dye
542 Reagent.

543 **Co-Culture Assay:** *Ptch1*$^{LacZ/LacZ}$;*Ptch2*$^{-/-}$ reporter cells were plated at a density of $1.4X10^5$ in 6-well
544 plates and transfected with *Gli-Luciferase*, *CMV-Renilla*, and with or without a variant of *Ptch1* 24

545 hours after plating. *Ptch1*$^{LacZ/LacZ}$;*Ptch2*$^{-/-}$ signaling cells were plated similarly and transfected with a
546 variant of Shh 24 hours after plating. Cells were then trypsinized and plated in 24-well plates in
547 specified combinations ($1.5x10^4$ of each type) 24 hours after transfections. Cells were grown to
548 confluency and switched to low serum medium (0.5% FBS) for 16 hours before assaying for
549 luciferase activity.

550 **Western Blots:** *Ptch1*$^{LacZ/LacZ}$;*Ptch2*$^{-/-}$ cells were transfected with Shh mutants as indicated. 48 hours
551 after transfection, *Ptch1*$^{LacZ/LacZ}$;*Ptch2*$^{-/-}$ cells were rinsed with PBS and lysed with RIPA buffer (150
552 mM NaCl, 50 mM Tris-Hcl, 1% Igepal, 0.5% Sodium Deoxycholate, and protease inhibitors) for 30
553 min on ice. Protein lysate was cleared by centrifugation at 13,000g for 30 min at 4 °C. 20 µg of each
554 sample was run on a 15% SDS-PAGE gel and transferred to a 0.45 micron nitrocellulose membrane.
555 Membranes were blocked with 5% milk in Tris-buffered saline with 0.1% Tween-20 (TBS-T) and
556 incubated with a rabbit polyclonal anti-Shh antibody (H160; Santa Cruz Biotechnology) at 1:250. A
557 goat anti-rabbit HRP-conjugated secondary antibody (Biorad) was used at 1:10000.

558

Acknowledgements: This work was supported by NIH grants R01GM097035 and 1R01GM117090 to HR. Vismodegib was a gift from Dr. de Sauvage (Genentech), *Dhh* and *Ihh* were a gift from Dr. Charles P. Emerson III (U. Mass. Med. School). Dr. A. Alfaro cloned the Shh binding mutants (E90A, H183A) and made the initial observation that they activate the Hh pathway *in vivo*. We thank Dr. M. Barro for her help with Western blotting, Dr. M. F. Bijlsma (AMC Amsterdam) for his help with the migration assays, and Dr. B. Roberts (Allen Institute for Cell Science) for his comments and advice. We also thank Fatma Ozguc for help with genome editing of the *Ptch1*$^{LacZ/LacZ}$;*Ptch2*$^{-/-}$;*Boc*$^{-/-}$;*Cdo*$^{-/-}$;*Gas1*$^{-/-}$;*Shh*$^{-/-}$ mESC line.

Author contributions: CC performed all experiments. HR and CC designed the experiments and wrote the manuscript.

References

Aanstad, P., Santos, N., Corbit, K.C., Scherz, P.J., Trinh le, A., Salvenmoser, W., Huisken, J., Reiter, J.F., and Stainier, D.Y. (2009). The extracellular domain of Smoothened regulates ciliary localization and is required for high-level Hh signaling. Curr. Biol. *19*, 1034–1039.

Alfaro, A.C., Roberts, B., Kwong, L., Bijlsma, M.F., and roelink, H. (2014). Ptch2 mediates the Shh response in Ptch1-/- cells. Development (Cambridge, England).

Allen, B.L., Song, J.Y., Izzi, L., Althaus, I.W., Kang, J.S., Charron, F., Krauss, R.S., and McMahon, A.P. (2011). Overlapping roles and collective requirement for the coreceptors GAS1, CDO, and BOC in SHH pathway function. Developmental Cell *20*, 775–787.

Bailey, J.M., Mohr, A.M., and Hollingsworth, M.A. (2009). Sonic hedgehog paracrine signaling regulates metastasis and lymphangiogenesis in pancreatic cancer. Oncogene *28*, 3513–3525.

Bale, A.E. (2002). Hedgehog signaling and human disease. Annu Rev Genomics Hum Genet *3*, 47–65.

Beachy, P.A., Karhadkar, S.S., and Berman, D.M. (2004). Tissue repair and stem cell renewal in carcinogenesis. Nature *432*, 324–331.

Bejsovec, A., and Wieschaus, E. (1993). Segment polarity gene interactions modulate epidermal patterning in Drosophila embryos. Development (Cambridge, England) *119*, 501–517.

Bhanot, P., Brink, M., Samos, C.H., Hsieh, J.C., Wang, Y., Macke, J.P., Andrew, D., Nathans, J., and Nusse, R. (1996). A new member of the frizzled family from Drosophila functions as a Wingless receptor. Nature *382*, 225–230.

Bijlsma, M.F., Damhofer, H., and roelink, H. (2012). Hedgehog-stimulated chemotaxis is mediated by smoothened located outside the primary cilium. Sci Signal *5*, ra60.

593 Briscoe, J., Chen, Y., Jessell, T.M., and Struhl, G. (2001). A hedgehog-insensitive form of patched
594 provides evidence for direct long-range morphogen activity of sonic hedgehog in the neural tube.
595 Molecular Cell *7*, 1279–1291.

596 Bumcrot, D.A., Takada, R., and McMahon, A.P. (1995a). Proteolytic processing yields two secreted
597 forms of sonic hedgehog. Mol. Cell. Biol. *15*, 2294–2303.

598 Bumcrot, D.A., Takada, R., and McMahon, A.P. (1995b). Proteolytic processing yields two secreted
599 forms of sonic hedgehog. Mol. Cell. Biol. *15*, 2294–2303.

600 Byrne, E.F.X., Sircar, R., Miller, P.S., Hedger, G., Luchetti, G., Nachtergaele, S., Tully, M.D.,
601 Mydock-McGrane, L., Covey, D.F., Rambo, R.P., et al. (2016). Structural basis of Smoothened
602 regulation by its extracellular domains. Nature *535*, 517–522.

603 Cermak, T., Doyle, E.L., Christian, M., Wang, L., Zhang, Y., Schmidt, C., Baller, J.A., Somia, N.V.,
604 Bogdanove, A.J., and Voytas, D.F. (2011). Efficient design and assembly of custom TALEN and
605 other TAL effector-based constructs for DNA targeting. Nucleic Acids Res. *39*, e82.

606 Chamberlain, C.E., Jeong, J., Guo, C., Allen, B.L., and McMahon, A.P. (2008). Notochord-derived
607 Shh concentrates in close association with the apically positioned basal body in neural target cells
608 and forms a dynamic gradient during neural patterning. Development (Cambridge, England) *135*,
609 1097–1106.

610 Chen, H.C. (2005). Boyden chamber assay. Methods in Molecular Biology (Clifton, N.J *294*, 15–22.

611 Chen, J.K., Taipale, J., Cooper, M.K., and Beachy, P.A. (2002a). Inhibition of Hedgehog signaling
612 by direct binding of cyclopamine to Smoothened. Genes & Development *16*, 2743–2748.

613 Chen, J.K., Taipale, J., Young, K.E., Maiti, T., and Beachy, P.A. (2002b). Small molecule
614 modulation of Smoothened activity. Proceedings of the National Academy of Sciences of the
615 United States of America *99*, 14071–14076.

616 Chen, M.H., Li, Y.J., Kawakami, T., Xu, S.M., and Chuang, P.T. (2004). Palmitoylation is required
617 for the production of a soluble multimeric Hedgehog protein complex and long-range signaling in
618 vertebrates. Genes Dev. *18*, 641–659.

619 Corbit, K.C., Aanstad, P., Singla, V., Norman, A.R., Stainier, D.Y., and Reiter, J.F. (2005).
620 Vertebrate Smoothened functions at the primary cilium. Nature *437*, 1018–1021.

621 Ericson, J., Morton, S., Kawakami, A., Roelink, H., and Jessell, T.M. (1996). Two critical periods of
622 Sonic Hedgehog signaling required for the specification of motor neuron identity. Cell *87*, 661–673.

623 Fuse, N., Maiti, T., Wang, B., Porter, J.A., Hall, T.M., Leahy, D.J., and Beachy, P.A. (1999). Sonic
624 hedgehog protein signals not as a hydrolytic enzyme but as an apparent ligand for patched.
625 Proceedings of the National Academy of Sciences of the United States of America *96*, 10992–
626 10999.

627 Gao, X., Arenas-Ramirez, N., Scales, S.J., and Hannoush, R.N. (2011). Membrane targeting of
628 palmitoylated Wnt and Hedgehog revealed by chemical probes. FEBS Letters *585*, 2501–2506.

629 García-Zaragoza, E., Pérez-Tavarez, R., Ballester, A., Lafarga, V., Jiménez-Reinoso, A., Ramírez,
630 A., Murillas, R., and Gallego, M.I. (2012). Intraepithelial paracrine Hedgehog signaling induces the
631 expansion of ciliated cells that express diverse progenitor cell markers in the basal epithelium of

632 the mouse mammary gland. Developmental Biology *372*, 28–44.

633 Goetz, J.A., Singh, S., Suber, L.M., Kull, F.J., and Robbins, D.J. (2006). A highly conserved amino-
634 terminal region of sonic hedgehog is required for the formation of its freely diffusible multimeric
635 form. J. Biol. Chem. *281*, 4087–4093.

636 Goodrich, L.V., Milenkovic, L., Higgins, K.M., and Scott, M.P. (1997). Altered neural cell fates and
637 medulloblastoma in mouse patched mutants. Science (New York, N.Y *277*, 1109–1113.

638 Gökhan, S., Song, Q., and Mehler, M.F. (1998). Generation and regulation of developing
639 immortalized neural cell lines. Methods *16*, 345–358.

640 Hamburger, V., and Hamilton, H.L. (1951). A series of normal stages in the development of the
641 chick embryo. J. Morphol. *88*, 49–90.

642 Hehr, U., Pineda-Alvarez, D.E., Uyanik, G., Hu, P., Zhou, N., Hehr, A., Schell-Apacik, C., Altus, C.,
643 Daumer-Haas, C., Meiner, A., et al. (2010). Heterozygous mutations in SIX3 and SHH are
644 associated with schizencephaly and further expand the clinical spectrum of holoprosencephaly.
645 Hum. Genet. *127*, 555–561.

646 Huang, P., Nedelcu, D., Watanabe, M., Jao, C., Kim, Y., Liu, J., and Salic, A. (2016). Cellular
647 Cholesterol Directly Activates Smoothened in Hedgehog Signaling. Cell *166*, 1176–1187.e14.

648 Incardona, J.P., Gruenberg, J., and Roelink, H. (2002). Sonic hedgehog induces the segregation of
649 patched and smoothened in endosomes. Curr. Biol. *12*, 983–995.

650 Incardona, J.P., Lee, J.H., Robertson, C.P., Enga, K., Kapur, R.P., and Roelink, H. (2000).
651 Receptor-mediated endocytosis of soluble and membrane-tethered Sonic hedgehog by Patched-1.
652 Proc. Natl. Acad. Sci. U.S.a. *97*, 12044–12049.

653 Ingham, P.W., and McMahon, A.P. (2001). Hedgehog signaling in animal development: paradigms
654 and principles. Genes & Development *15*, 3059–3087.

655 Itasaki, N., Bel-Vialar, S., and Krumlauf, R. (1999). “Shocking” developments in chick embryology:
656 electroporation and in ovo gene expression. Nature Cell Biology *1*, E203–E207.

657 Izzi, L., Levesque, M., Morin, S., Laniel, D., Wilkes, B.C., Mille, F., Krauss, R.S., McMahon, A.P.,
658 Allen, B.L., and Charron, F. (2011). Boc and Gas1 each form distinct Shh receptor complexes with
659 Ptch1 and are required for Shh-mediated cell proliferation. Developmental Cell *20*, 788–801.

660 Janda, C.Y., Waghray, D., Levin, A.M., Thomas, C., and Garcia, K.C. (2012). Structural basis of
661 Wnt recognition by Frizzled. Science (New York, N.Y *337*, 59–64.

662 Kawakami, A., Kimura Kawakami, M., Nomura, T., and Fujisawa, H. (1997). Distributions of PAX6
663 and PAX7 proteins suggest their involvement in both early and late phases of chick brain
664 development. Mechanisms of Development *66*, 119–130.

665 Kristiansen, K. (2004). Molecular mechanisms of ligand binding, signaling, and regulation within
666 the superfamily of G-protein-coupled receptors: molecular modeling and mutagenesis approaches
667 to receptor structure and function. Pharmacol Ther *103*, 21–80.

668 Lee, Y., Miller, H.L., Russell, H.R., Boyd, K., Curran, T., and McKinnon, P.J. (2006). Patched2
669 modulates tumorigenesis in patched1 heterozygous mice. Cancer Research *66*, 6964–6971.

670 Mao, J., Ligon, K.L., Rakhlin, E.Y., Thayer, S.P., Bronson, R.T., Rowitch, D., and McMahon, A.P.
671 (2006). A novel somatic mouse model to survey tumorigenic potential applied to the Hedgehog
672 pathway. Cancer Research *66*, 10171–10178.

673 Marigo, V., Davey, R.A., Zuo, Y., Cunningham, J.M., and Tabin, C.J. (1996). Biochemical evidence
674 that patched is the Hedgehog receptor. Nature *384*, 176–179.

675 Meyer, N.P., and Roelink, H. (2003). The amino-terminal region of Gli3 antagonizes the Shh
676 response and acts in dorsoventral fate specification in the developing spinal cord. Developmental
677 Biology *257*, 343–355.

678 Milenkovic, L., Scott, M.P., and Rohatgi, R. (2009). Lateral transport of Smoothened from the
679 plasma membrane to the membrane of the cilium. The Journal of Cell Biology *187*, 365–374.

680 Myers, B.R., Sever, N., Chong, Y.C., Kim, J., Belani, J.D., Rychnovsky, S., Bazan, J.F., and
681 Beachy, P.A. (2013). Hedgehog pathway modulation by multiple lipid binding sites on the
682 smoothened effector of signal response. Developmental Cell *26*, 346–357.

683 Nachtergaele, S., Whalen, D.M., Mydock, L.K., Zhao, Z., Malinauskas, T., Krishnan, K., Ingham,
684 P.W., Covey, D.F., Siebold, C., and Rohatgi, R. (2013). Structure and function of the Smoothened
685 extracellular domain in vertebrate Hedgehog signaling. Elife *2*, e01340.

686 Nedelcu, D., Liu, J., Xu, Y., Jao, C., and Salic, A. (2013). Oxysterol binding to the extracellular
687 domain of Smoothened in Hedgehog signaling. Nature Chemical Biology.

688 Nikaido, H., and Zgurskaya, H.I. (2001). AcrAB and related multidrug efflux pumps of Escherichia
689 coli. Journal of Molecular Microbiology and Biotechnology *3*, 215–218.

690 Nikaido, H., and Takatsuka, Y. (2009). Mechanisms of RND multidrug efflux pumps. Biochimica Et
691 Biophysica Acta *1794*, 769–781.

692 Okada, A., Charron, F., Morin, S., Shin, D.S., Wong, K., Fabre, P.J., Tessier-Lavigne, M., and
693 McConnell, S.K. (2006). Boc is a receptor for sonic hedgehog in the guidance of commissural
694 axons. Nature *444*, 369–373.

695 Pepinsky, R.B., Zeng, C., Wen, D., Rayhorn, P., Baker, D.P., Williams, K.P., Bixler, S.A., Ambrose,
696 C.M., Garber, E.A., Miatkowski, K., et al. (1998). Identification of a palmitic acid-modified form of
697 human Sonic hedgehog. The Journal of Biological Chemistry *273*, 14037–14045.

698 Porter, J.A., Young, K.E., and Beachy, P.A. (1996). Cholesterol modification of hedgehog signaling
699 proteins in animal development. Science (New York, N.Y *274*, 255–259.

700 Ramirez-Weber, F.A., Casso, D.J., Aza-Blanc, P., Tabata, T., and Kornberg, T.B. (2000).
701 Hedgehog signal transduction in the posterior compartment of the Drosophila wing imaginal disc.
702 Molecular Cell *6*, 479–485.

703 Ran, F.A., Hsu, P.D., Wright, J., Agarwala, V., Scott, D.A., and Zhang, F. (2013). Genome
704 engineering using the CRISPR-Cas9 system. Nat Protoc *8*, 2281–2308.

705 Rebollido-Rios, R., Bandari, S., Wilms, C., Jakuschev, S., Vortkamp, A., Grobe, K., and Hoffmann,
706 D. (2014). Signaling domain of Sonic Hedgehog as cannibalistic calcium-regulated zinc-peptidase.
707 PLoS Comput. Biol. *10*, e1003707.

708 Roberts, B., Casillas, C., Alfaro, A.C., Jägers, C., and roelink, H. (2016). Patched1 and Patched2
709 inhibit Smoothened non-cell autonomously. Elife *5*, e17634.

710 Roelink, H., Porter, J.A., Chiang, C., Tanabe, Y., Chang, D.T., Beachy, P.A., and Jessell, T.M.
711 (1995). Floor plate and motor neuron induction by different concentrations of the amino-terminal
712 cleavage product of sonic hedgehog autoproteolysis. Cell *81*, 445–455.

713 Roessler, E., El-Jaick, K.B., Dubourg, C., Vélez, J.I., Solomon, B.D., Pineda-Alvarez, D.E.,
714 Lacbawan, F., Zhou, N., Ouspenskaia, M., Paulussen, A., et al. (2009). The mutational spectrum of
715 holoprosencephaly-associated changes within the SHH gene in humans predicts loss-of-function
716 through either key structural alterations of the ligand or its altered synthesis. Hum. Mutat. *30*,
717 E921–E935.

718 Rohatgi, R., Milenkovic, L., and Scott, M.P. (2007). Patched1 regulates hedgehog signaling at the
719 primary cilium. Science (New York, N.Y *317*, 372–376.

720 Rudin, C.M. (2012). Vismodegib. Clin. Cancer Res. *18*, 3218–3222.

721 Ryan, A.K., Blumberg, B., Rodriguez-Esteban, C., Yonei-Tamura, S., Tamura, K., Tsukui, T., la
722 Peña, de, J., Sabbagh, W., Greenwald, J., Choe, S., et al. (1998). Pitx2 determines left-right
723 asymmetry of internal organs in vertebrates. Nature *394*, 545–551.

724 Sasaki, H., Hui, C., Nakafuku, M., and Kondoh, H. (1997). A binding site for Gli proteins is essential
725 for HNF-3beta floor plate enhancer activity in transgenics and can respond to Shh in vitro.
726 Development (Cambridge, England) *124*, 1313–1322.

727 Singh, S., Tokhunts, R., Baubet, V., Goetz, J.A., Huang, Z.J., Schilling, N.S., Black, K.E.,
728 MacKenzie, T.A., Dahmane, N., and Robbins, D.J. (2009). Sonic hedgehog mutations identified in
729 holoprosencephaly patients can act in a dominant negative manner. Hum. Genet. *125*, 95–103.

730 Taipale, J., Cooper, M.K., Maiti, T., and Beachy, P.A. (2002). Patched acts catalytically to suppress
731 the activity of Smoothened. Nature *418*, 892–897.

732 Tenzen, T., Allen, B.L., Cole, F., Kang, J.S., Krauss, R.S., and McMahon, A.P. (2006). The cell
733 surface membrane proteins Cdo and Boc are components and targets of the Hedgehog signaling
734 pathway and feedback network in mice. Developmental Cell *10*, 647–656.

735 Tian, H., Callahan, C.A., DuPree, K.J., Darbonne, W.C., Ahn, C.P., Scales, S.J., and de Sauvage,
736 F.J. (2009). Hedgehog signaling is restricted to the stromal compartment during pancreatic
737 carcinogenesis. Proceedings of the National Academy of Sciences of the United States of America
738 *106*, 4254–4259.

739 Traiffort, E., Dubourg, C., Faure, H., Rognan, D., Odent, S., Durou, M.-R., David, V., and Ruat, M.
740 (2004). Functional characterization of sonic hedgehog mutations associated with
741 holoprosencephaly. J. Biol. Chem. *279*, 42889–42897.

742 Tukachinsky, H., Petrov, K., Watanabe, M., and Salic, A. (2016). Mechanism of inhibition of the
743 tumor suppressor Patched by Sonic Hedgehog. Proceedings of the National Academy of Sciences
744 of the United States of America *113*, E5866–E5875.

745 Wang, Y., and McMahon, A.P. (2013). A novel site comes into sight. Elife *2*, e01680.

746 Wichterle, H., Lieberam, I., Porter, J.A., and Jessell, T.M. (2002). Directed differentiation of

747 embryonic stem cells into motor neurons. Cell *110*, 385–397.

748 Xie, J., Murone, M., Luoh, S.M., Ryan, A., Gu, Q., Zhang, C., Bonifas, J.M., Lam, C.W., Hynes, M.,
749 Goddard, A., et al. (1998). Activating Smoothened mutations in sporadic basal-cell carcinoma.
750 Nature *391*, 90–92.

751 Yang, Y., Drossopoulou, G., Chuang, P.T., Duprez, D., Marti, E., Bumcrot, D., Vargesson, N.,
752 Clarke, J., Niswander, L., McMahon, A., et al. (1997). Relationship between dose, distance and
753 time in Sonic Hedgehog-mediated regulation of anteroposterior polarity in the chick limb.
754 Development (Cambridge, England) *124*, 4393–4404.

755 Zhang, J., Rosenthal, A., de Sauvage, F.J., and Shivdasani, R.A. (2001a). Downregulation of
756 Hedgehog signaling is required for organogenesis of the small intestine in Xenopus.
757 Developmental Biology *229*, 188–202.

758 Zhang, X.M., Ramalho-Santos, M., and McMahon, A.P. (2001b). Smoothened mutants reveal
759 redundant roles for Shh and Ihh signaling including regulation of L/R asymmetry by the mouse
760 node. Cell *105*, 781–792.

761

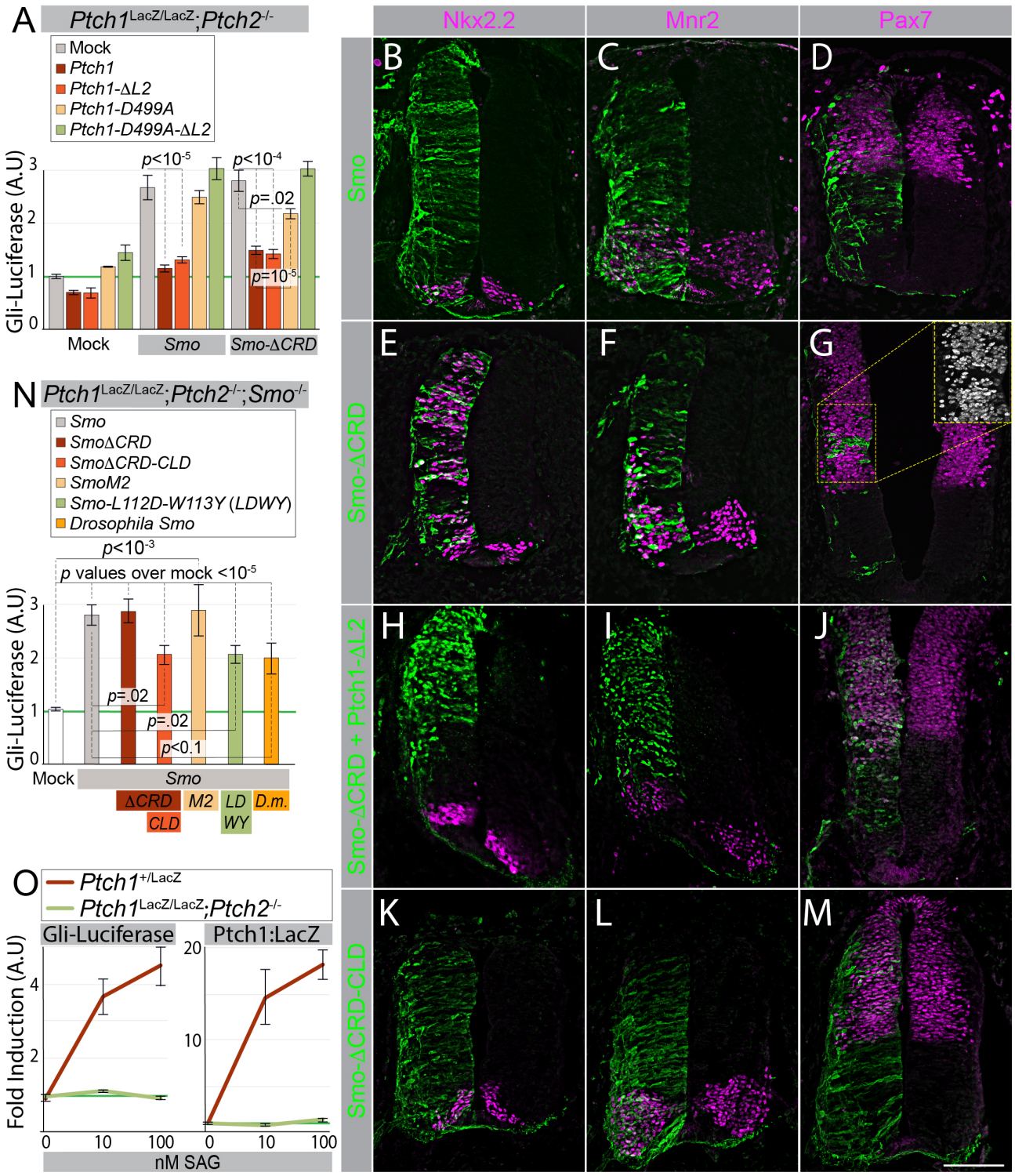

Figure 1. SmoΔCRD retains sensitivity to Ptch1-mediated inhibition in vitro and in vivo

(A) *Ptch1*$^{LacZ/LacZ}$;*Ptch2*$^{-/-}$ cells were co-transfected with *Gli-luc* and *GFP* (Mock), *Ptch1*, *Ptch1-ΔL2*, *Ptch1-D499A*, or *Ptch1ΔL2-D499A*; or *Gli-luc*, *Smo*, and *GFP*, *Ptch1*, *Ptch1-ΔL2*, *Ptch1D499A*, or

766 *Ptch1-ΔL2-D499A*; or *Gli-luc*, *Smo-ΔCRD* and *GFP*, *Ptch1*, *Ptch1-ΔL2*, *Ptch1-D499A*, or *Ptch1-ΔL2-*
767 *D499A*. Luciferase levels in *Gli-luc* Mock transfected *Ptch1*$^{LacZ/LacZ}$;*Ptch2*$^{-/-}$ cells were arbitrarily set at
768 "1". (B-M) Cross-sections of stage 20 HH chicken neural tubes electroporated with *Smo* (B-D), *Smo-*
769 *ΔCRD* (E-G), *Smo-ΔCRD* + *Ptch1-ΔL2* (1:1) (H-J), or *Smo-ΔCRD-CLD* (K-M) labeled in green.
770 Sections are stained with antibodies to Nkx2.2 (B, E, H, K), Mnr2 (C, F, I, L), and Pax7 (D, G, J, M)
771 labeled in magenta. Insert in G shows Pax7 staining. Scale bar is 100μm. (N) *Ptch1*$^{LacZ/LacZ}$;*Ptch2*$^{-/-}$
772 ;*Smo*$^{-/-}$ fibroblasts were co-transfected with *Gli-luc* and the indicated Smo variant. Luciferase levels
773 in *Gli-luc* Mock transfected *Ptch1*$^{LacZ/LacZ}$;*Ptch2*$^{-/-}$;*Smo*$^{-/-}$ cells were arbitrarily set at "1". (O) SAG dose-
774 response in *Ptch1*$^{+/LacZ}$ and *Ptch1*$^{LacZ/LacZ}$;*Ptch2*$^{-/-}$. The Hh response was measured by transfected
775 *Gli-luc*, or by measuring LacZ levels from the *Ptch1:LacZ* allele. Pathway activation in the absence
776 of SAG was set at "1". All error bars are s.e.m., *p* values (Student T-test, 2 tailed) are indicated were
777 relevant, (A) n≥4, (N) n≥4, (O) n≥4, all independent biological replicates.

778

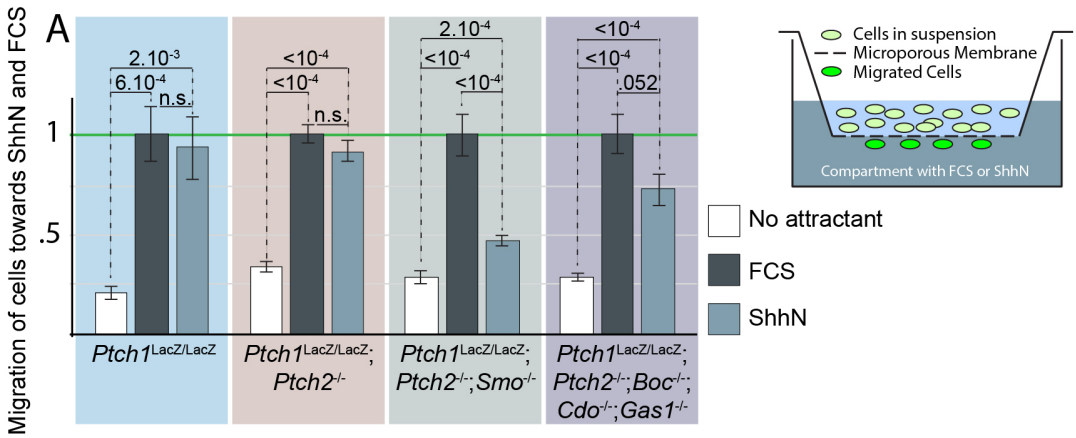
A
Migration of cells towards ShhN and FCS
2.10-3
6.10-4
n.s.
<10-4
<10-4
n.s.
2.10-4
<10-4
<10-4
<10-4
<10-4
.052
1
.5
Ptch1LacZ/LacZ
Ptch1LacZ/LacZ; Ptch2-/-
Ptch1LacZ/LacZ; Ptch2-/-;Smo-/-
Ptch1LacZ/LacZ; Ptch2-/-;Boc-/-; Cdo-/-;Gas1-/-
Cells in suspension
Microporous Membrane
Migrated Cells
Compartment with FCS or ShhN
No attractant
FCS
ShhN

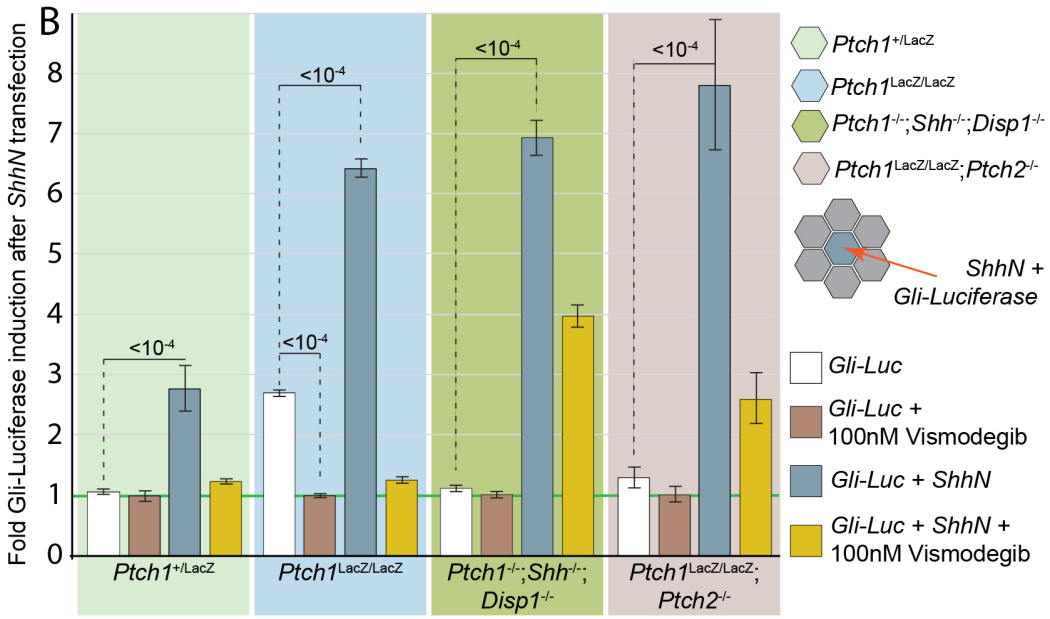
B
Fold Gli-Luciferase induction after ShhN transfection
<10-4
<10-4
<10-4
<10-4
<10-4
<10-4
0
1
2
3
4
5
6
7
8
Ptch1+/LacZ
Ptch1LacZ/LacZ
Ptch1-/-;Shh-/-;Disp1-/-
Ptch1LacZ/LacZ; Ptch2-/-
Ptch1+/LacZ
Ptch1LacZ/LacZ
Ptch1-/-;Shh-/-;Disp1-/-
Ptch1LacZ/LacZ;Ptch2-/-
ShhN + Gli-Luciferase
Gli-Luc
Gli-Luc + 100nM Vismodegib
Gli-Luc + ShhN
Gli-Luc + ShhN + 100nM Vismodegib

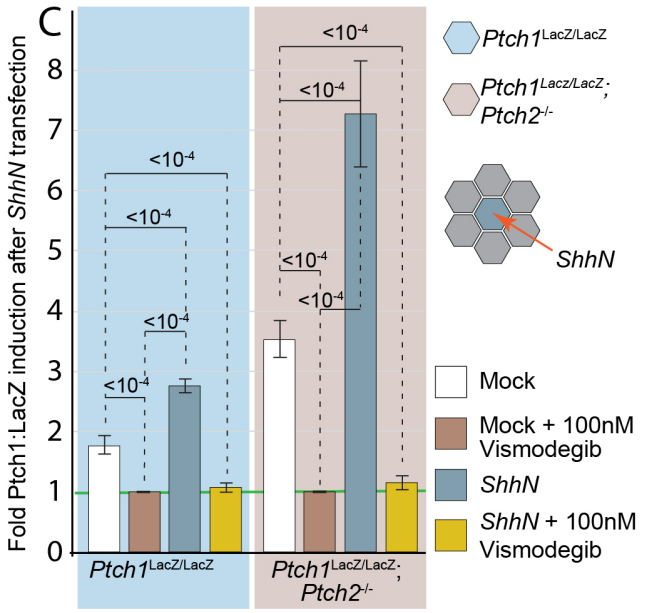
C
Fold Ptch1:LacZ induction after ShhN transfection
<10-4
<10-4
<10-4
<10-4
<10-4
<10-4
<10-4
<10-4
0
1
2
3
4
5
6
7
8
Ptch1LacZ/LacZ
Ptch1LacZ/LacZ; Ptch2-/-
Ptch1LacZ/LacZ
Ptch1LacZ/LacZ; Ptch2-/-
ShhN
Mock
Mock + 100nM Vismodegib
ShhN
ShhN + 100nM Vismodegib

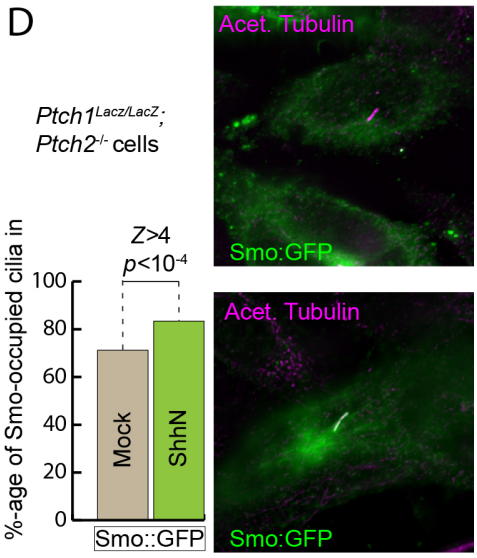
D
Ptch1Lacz/LacZ; Ptch2-/- cells
Acet. Tubulin
Smo:GFP
Z>4
p<10-4
%-age of Smo-occupied cilia in
100
80
60
40
20
0
Mock
ShhN
Smo::GFP
Acet. Tubulin
Smo:GFP

780 **Figure 2. Activation of the Hh response by ShhN does not require Ptch1/2 activity**

781 (A) Cells with the indicated genotypes were assayed in a modified Boyden chamber (diagram) for
782 their ability to migrate towards FCS or ShhN. Migration was normalized to FCS for each condition.
783 (B) *Ptch1*$^{+/LacZ}$ cells, *Ptch1*$^{LacZ/LacZ}$ cells, *Ptch1*$^{-/-}$;*Shh*$^{-/-}$;*Disp1*$^{-/-}$, and *Ptch1*$^{LacZ/LacZ}$;*Ptch2*$^{-/-}$ cells
784 (indicated) were co-transfected with *Gli-Luc* and *GFP* (Mock; white/brown bars) or co-transfected
785 with *Gli-Luc* and *ShhN* (blue/yellow bars). Each condition was treated with either a Smo inhibitor,
786 100 nM Vismodegib (brown/yellow bars), or a DMSO vehicle control (white/blue bars). Luciferase
787 levels in mock transfected cells treated with 100 nM Vismodegib for each cell line were set at "1".
788 (C) *Ptch1*$^{LacZ/LacZ}$ cells and *Ptch1*$^{LacZ/LacZ}$;*Ptch2*$^{-/-}$ (indicated) were assessed for Ptch1:LacZ expression
789 after mock transfection (white/brown bars) or *ShhN* transfection (blue/yellow bars). Each condition
790 was treated with either a Smo inhibitor, 100 nM Vismodegib (brown/yellow bars), or a DMSO vehicle
791 control (white/blue bars). Luciferase levels in mock transfected cells treated with 100 nM Vismodegib
792 for each cell line were set at "1". (D) Cilial localization of Smo::GFP was quantified in Mock and *ShhN*
793 transfected *Ptch1*$^{LacZ/LacZ}$;*Ptch2*$^{-/-}$ cells. Over 300 Smo::GFP co-expressing cells were assessed for
794 each condition. Z (standard) score>4, *p*-value is $<10^{-4}$. All error bars are s.e.m., *p* values (Student T-
795 test, 1 tailed) are indicated were relevant, (A) n≥4, (B) n≥9, (C) n≥13, all independent biological
796 replicates.

797

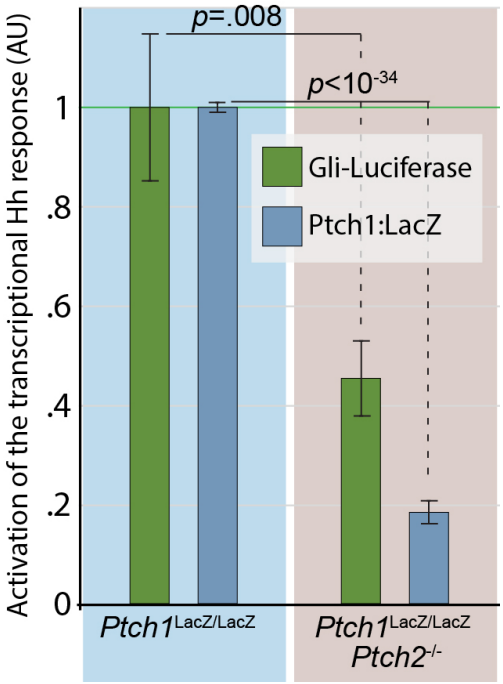

Figure 2, Figure Supplement 1. Intrinsic levels of Hh pathway activation in *Ptch1*$^{LacZ/LacZ}$ and *Ptch1*$^{LacZ/LacZ}$;*Ptch2*$^{-/-}$ cells. Hh pathway activation in *Ptch1*$^{LacZ/LacZ}$ and *Ptch1*$^{LacZ/LacZ}$;*Ptch2*$^{-/-}$ was measured in parallel using *Gli-luc* and *Ptch1:LacZ.* Using both methods we find higher Hh pathway activation in the *Ptch1*$^{LacZ/LacZ}$ cells than the *Ptch1*$^{LacZ/LacZ}$;*Ptch2*$^{-/-}$ cells. Luciferase and LacZ levels in *Ptch1*$^{LacZ/LacZ}$ cells were set at "1". Error bars are s.e.m., *p*-values (Student t-test, 2 tailed) are indicated were relevant, n=6 for Gli-Luc assay, n≥25 for LacZ assay, all independent biological replicates.

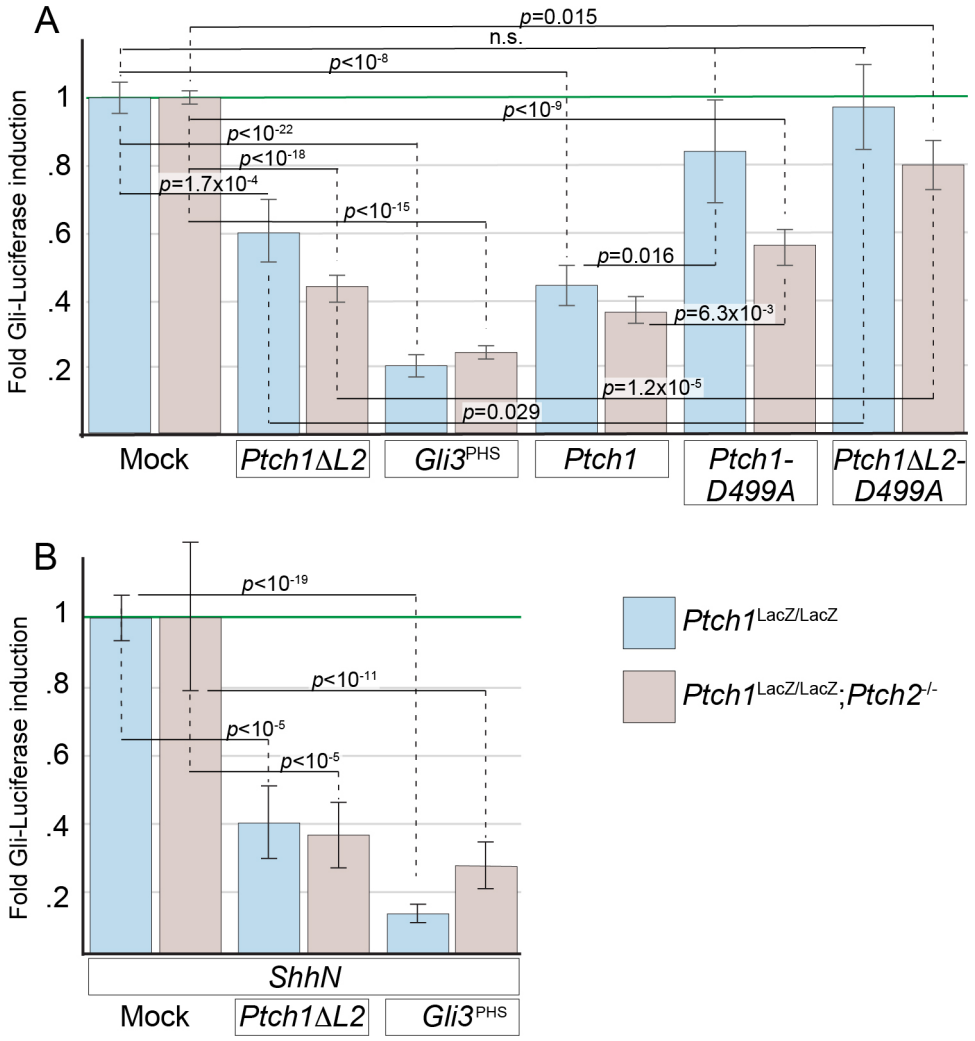

806

807

808 **Figure 2, Figure Supplement 2. Ptch1-mediated inhibition of the Hh response is similar in**
809 ***Ptch1$^{LacZ/LacZ}$* and *Ptch1$^{LacZ/LacZ}$;Ptch2$^{-/-}$* cells.** (A) Gli-luc levels were assayed in *Ptch1$^{LacZ/LacZ}$*
810 (blue bars) and *Ptch1$^{LacZ/LacZ}$;Ptch2$^{-/-}$* (pink bars) transfected with *Ptch1*, *Ptch1ΔL2*, *Ptch1-D499A*,
811 *Ptch1ΔL2-D499A* (indicated) or a dominant inhibitory form of *Gli3* (*Gli3^{phs}*) together with *Gli-luc*.
812 Luciferase levels in *Gli-Luc* Mock transfected cells were set at "1" for each cell line. (B) Gli-luc
813 levels were assayed in *Ptch1$^{LacZ/LacZ}$* (blue bars) and *Ptch1$^{LacZ/LacZ}$;Ptch2$^{-/-}$* (pink bars) transfected
814 with *Ptch1ΔL2,or Gli3^{phs}* together with *Gli-luc* and *ShhN*. Luciferase levels in *ShhN*, Mock co-
815 transfected cells were set at "1" for each cell line. All error bars are s.e.m., *p*-values (Student t-test,
816 2 tailed) are indicated were relevant, (A) n≥4, (B) n≥11, all independent biological replicates.

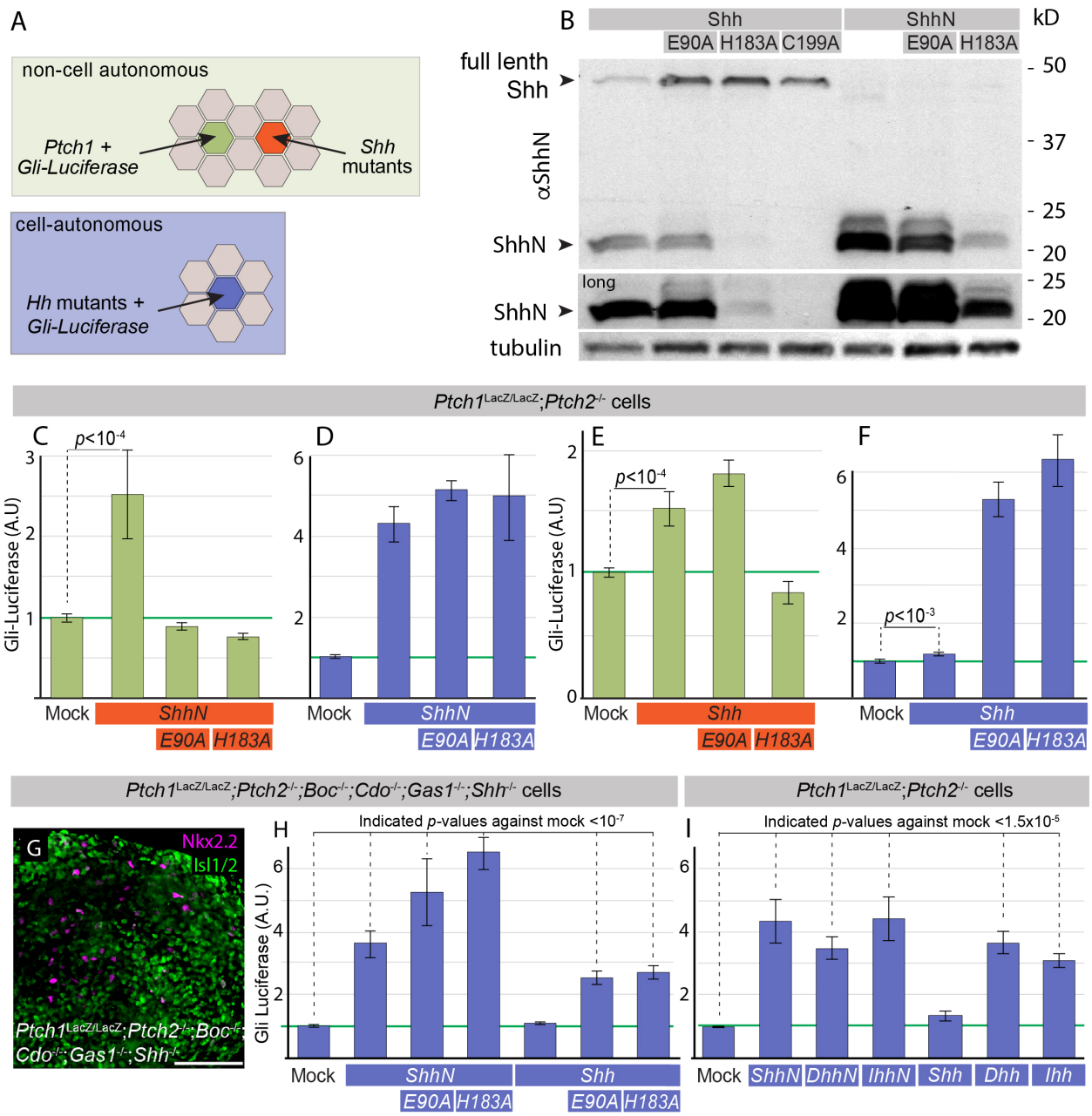

Figure 3. Shh mutants activate the Hh pathway cell-autonomously in cells lacking Hh receptors

(A) Diagram of non-cell autonomous signaling (green background): *Ptch1*$^{LacZ/LacZ}$;*Ptch2*$^{-/-}$ reporter cells transfected with *Gli-Luc* and *Ptch1* (green hexagons) were grown in a 1:1 mixed co-culture of *GFP* (Mock) transfected or *Shh* mutant transfected *Ptch1*$^{LacZ/LacZ}$;*Ptch2*$^{-/-}$ cells (red hexagons). Diagram of cell-autonomous signaling (purple background): *Ptch1*$^{LacZ/LacZ}$;*Ptch2*$^{-/-}$ cells transfected with *Gli-Luc* alone (Mock) or co-transfected with *Shh* mutants. (B) Western blot analysis of Shh, Shh-E90A, Shh-H183A, Shh-C199A, ShhN, ShhN-E90A, and ShhN-H183A protein expression in

827 *Ptch1*$^{LacZ/LacZ}$;*Ptch2*$^{-/-}$ cells, using an antibody directed against the N-terminal domain of Shh. (C)
828 *Ptch1*$^{LacZ/LacZ}$;*Ptch2*$^{-/-}$ reporter cells co-transfected with *Gli-Luc* and *Ptch1* were co-cultured with mock,
829 *ShhN*, *ShhN-E90A*, or *ShhN-H183A* transfected *Ptch1*$^{LacZ/LacZ}$;*Ptch2*$^{-/-}$ cells. Luciferase levels in
830 *Ptch1*$^{LacZ/LacZ}$;*Ptch2*$^{-/-}$ reporter cells co-cultured with mock transfected cells were set at "1". (D)
831 *Ptch1*$^{LacZ/LacZ}$;*Ptch2*$^{-/-}$ cells were transfected with *Gli-Luc* alone (Mock) or co-transfected with *Gli-Luc*
832 and *ShhN*, *ShhN-E90A*, or *ShhN-H183A*. Luciferase levels in mock transfected *Ptch1*$^{LacZ/LacZ}$;*Ptch2*$^{-}$
833 $^{/-}$ cells were set at "1". (E) *Ptch1*$^{LacZ/LacZ}$;*Ptch2*$^{-/-}$ reporter cells co-transfected with *Gli-Luc* and *Ptch1*
834 were co-cultured with mock, *Shh*, *Shh-E90A*, or *Shh-H183A* transfected *Ptch1*$^{LacZ/LacZ}$;*Ptch2*$^{-/-}$ cells.
835 Luciferase levels in *Ptch1*$^{LacZ/LacZ}$;*Ptch2*$^{-/-}$ reporter cells co-cultured with mock transfected cells were
836 set at "1". (F) *Ptch1*$^{LacZ/LacZ}$;*Ptch2*$^{-/-}$ cells were transfected with *Gli-Luc* alone (Mock) or co-transfected
837 with *Gli-Luc* and *Shh*, *Shh-E90A*, or *Shh-H183A*. Luciferase levels in mock transfected
838 *Ptch1*$^{LacZ/LacZ}$;*Ptch2*$^{-/-}$ cells were set at "1". (G) Neuralized Embryoid body derived from
839 *Ptch1*$^{LacZ/LacZ}$;*Ptch2*$^{-/-}$;*Boc*$^{-/-}$;*Cdo*$^{-/-}$;*Gas1*$^{-/-}$;*Shh*$^{-/-}$ mESCs. Expression of Nkx2.2 and Olig2 was
840 assessed by immunofluorescence after 5 days in culture. (H) *Ptch1*$^{LacZ/LacZ}$;*Ptch2*$^{-/-}$;*Boc*$^{-/-}$;*Cdo*$^{-/-}$;*Gas1*$^{-}$
841 $^{/-}$;*Shh*$^{-/-}$ cells were transfected with *Gli-Luc* alone (Mock) or co-transfected with *Gli-Luc* and *Shh*, *Shh-*
842 *E90A*, *Shh-H183A*, *ShhN*, *ShhN-E90A*, or *ShhN-H183A*. Luciferase levels in Mock transfected cells
843 were set at "1". (I) *Ptch1*$^{LacZ/LacZ}$;*Ptch2*$^{-/-}$ cells were transfected with *Gli-Luc* alone (Mock) or co-
844 transfected with *Gli-Luc* and *ShhN*, *DhhN*, *IhhN*, *Shh*, *Dhh*, *or Ihh.* Luciferase levels in Mock
845 transfected cells were set at "1". All error bars are s.e.m., *p* values (Student t-test, 2 tailed) against
846 mock are indicated were relevant, (C) n≥11, (D) n≥25, (E) n≥6, (F) n≥34, (H) n≥4, (I) n≥6, all
847 independent biological replicates.

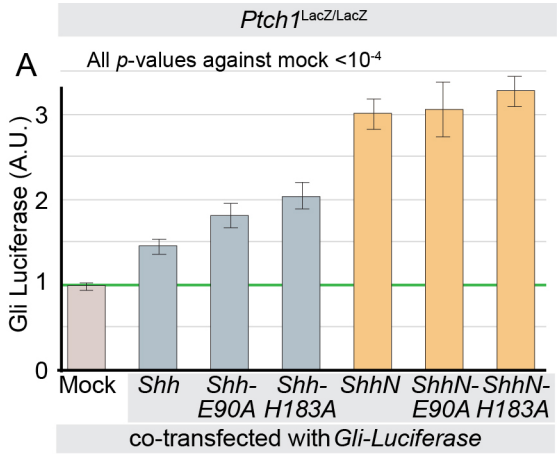

848

849

850 **Figure 3, Figure Supplement 1. *Ptch1*$^{LacZ/LacZ}$*;Ptch2*$^{-/-}$cells activate the Hh response after**
851 **transfection with Shh mutants** (A) *Ptch1*$^{LacZ/LacZ}$ cells were transfected with *Gli-Luc* alone (Mock)
852 or co-transfected with *Gli-Luc* and *Shh*, *Shh-E90A*, *Shh-H183*, *ShhN*, *ShhN-E90A*, or *ShhN-H183A*.
853 Luciferase levels in mock transfected *Ptch1*$^{LacZ/LacZ}$ cells were set at "1". All error bars are s.e.m., *p*
854 values (Student T-test, 2 tailed) are indicated were relevant, n≥5, all independent biological
855 replicates.

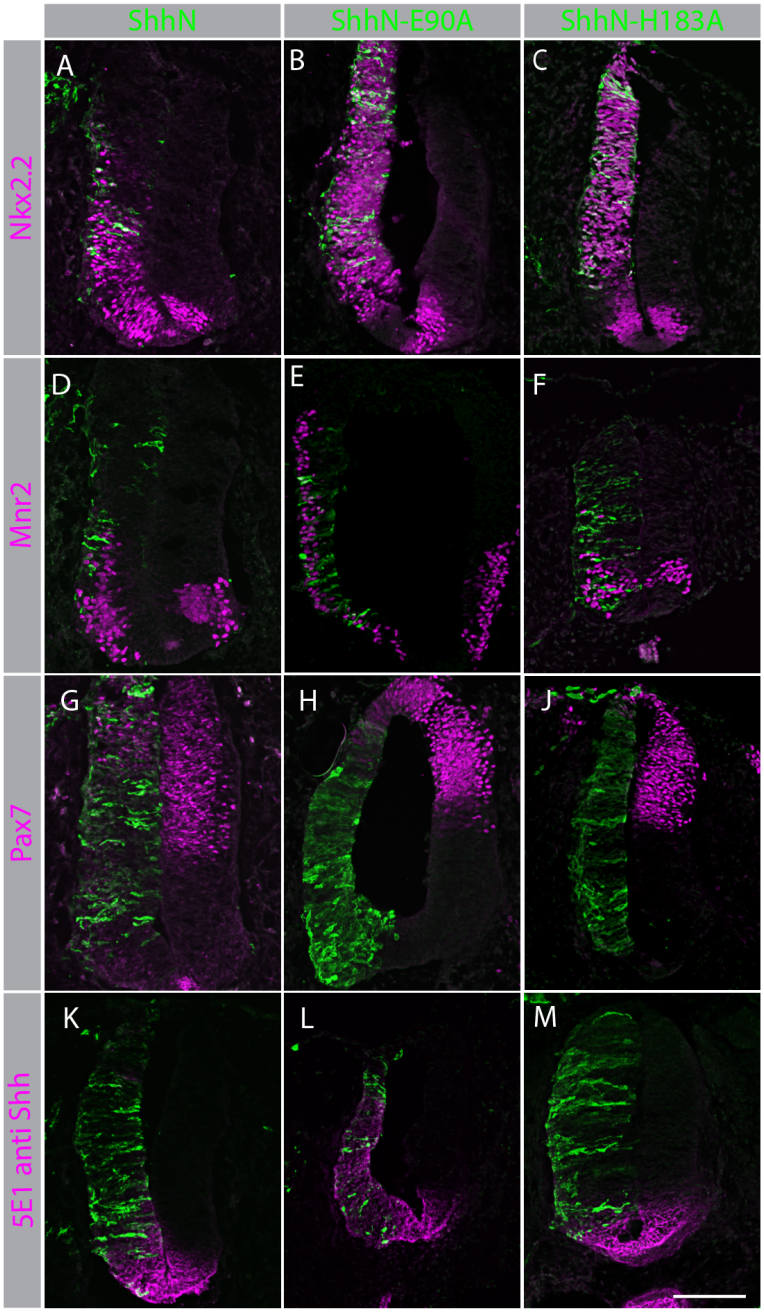

Figure 4. ShhN mutants cell-autonomously activate the Hh pathway *in vivo* independent of extracellular receptor binding

(A-M) Cross-sections of stage 20 HH chicken neural tubes co-electroporated at stage 10 with *GFP* and *ShhN* (A,D,G,K), *ShhN-E90A* (B,E,H,L), or *ShhN-H183A* (C,F,J,M) labeled in green. Sections are stained with antibodies to Nkx2.2 (A-C), Mnr2 (D-F), Pax7 (G-J), and Shh (5E1) (K-M) labeled in magenta. Scale bar is 100μm.

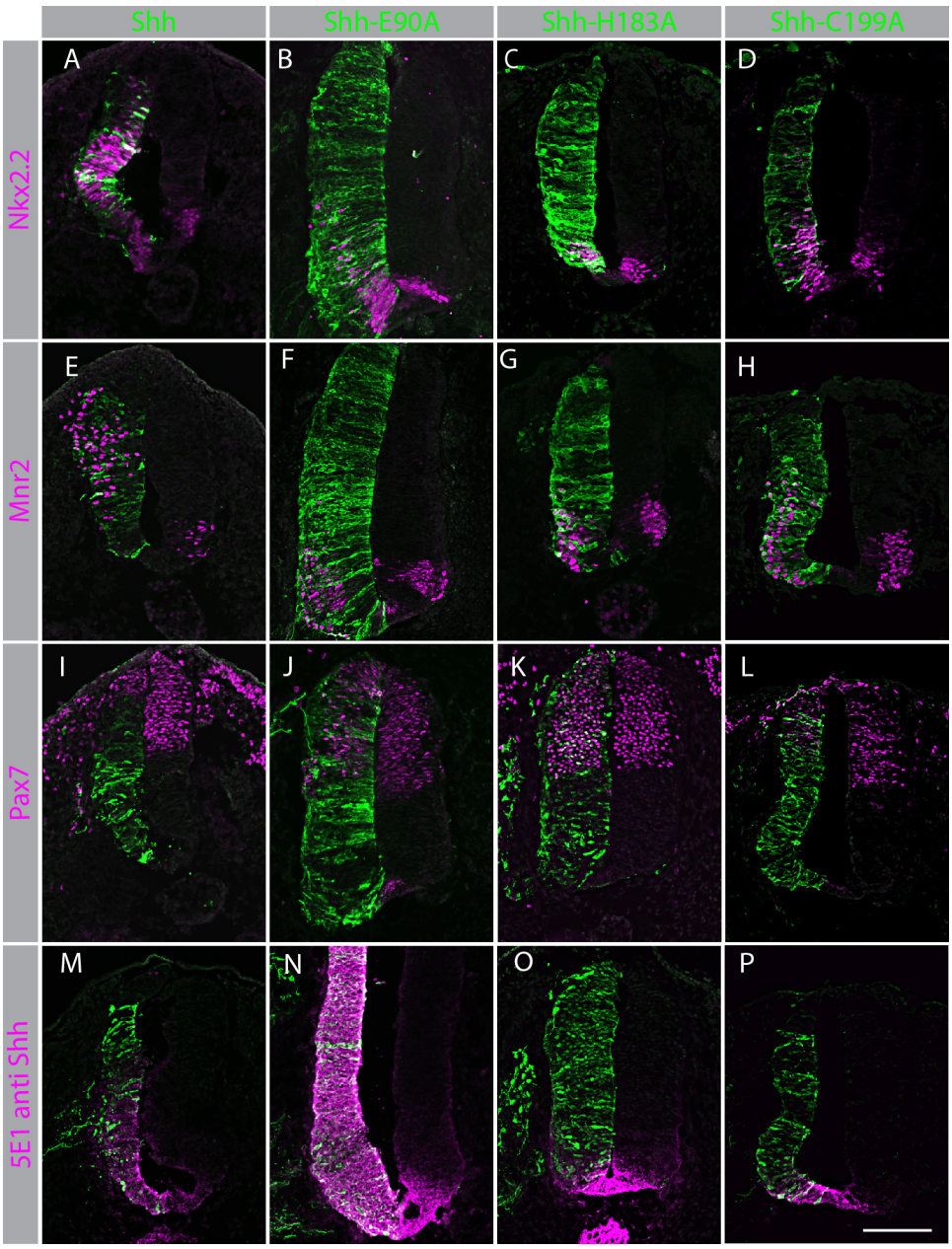

Figure 5. Shh mutants cell-autonomously activate the Hh pathway *in vivo* independent of extracellular receptor binding and despite lack of autoproteolytic processing

(A-P) Cross-sections of stage 20 HH chicken neural tubes co-electroporated with *GFP* and *Shh* (A, E, I, M), *Shh-E90A* (B, F, J, N), *Shh-H183A* (C, G, K, O), or *Shh-C199A* (*C199Ah* (D, H, L, P), labeled in green). Sections are stained with antibodies to Nkx2.2 (A-D), Mnr2 (E-H), Pax7 (I-L), and Shh (5E1) (M-P) labeled in magenta. Scale bar is 100μm.

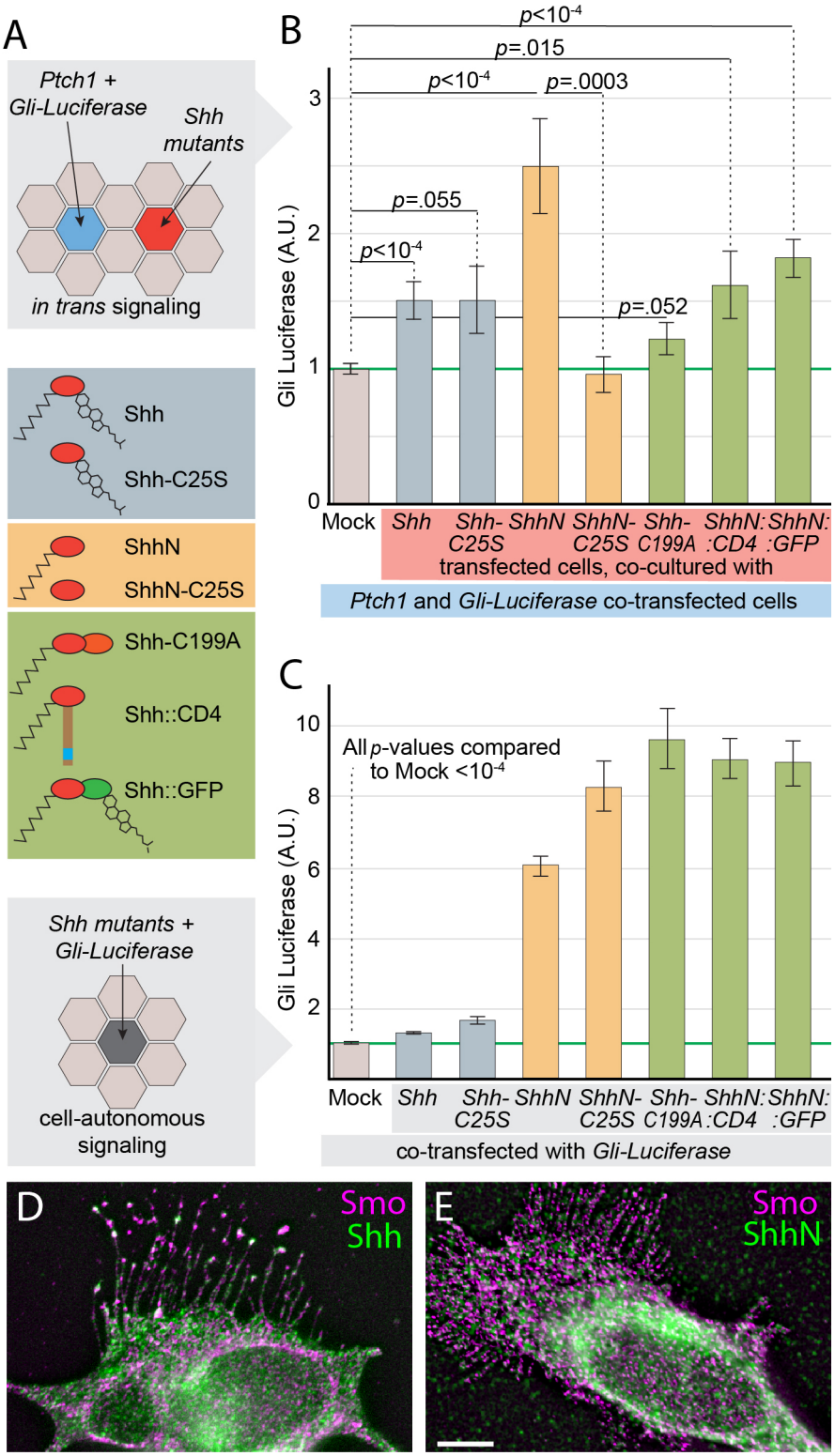

871

872

873

874

875 **Figure 6. The cholesterol modification of Shh impedes cell-autonomous Hh pathway**
876 **activation**

877 (A) Diagram of non-cell autonomous signaling (top): *Ptch1*$^{LacZ/LacZ}$;*Ptch2*$^{-/-}$ reporter cells transfected
878 with *Gli-Luc* and *Ptch1* (blue hexagons) were grown in a 1:1 mixed co-culture of *GFP* (Mock)
879 transfected or *Shh* (mutant) transfected *Ptch1*$^{LacZ/LacZ}$;*Ptch2*$^{-/-}$ cells (red hexagons). Cell-autonomous
880 signaling experimental design (bottom): *Ptch1*$^{LacZ/LacZ}$;*Ptch2*$^{-/-}$ cells co-transfected with *Gli-Luc* and
881 *GFP* (Mock) transfected or co-transfected with *Gli-Luc* and *Shh* (mutants). Diagram of Shh (mutants)
882 with varying lipophilic an C-terminal modifications (middle). (B) *Ptch1*$^{LacZ/LacZ}$;*Ptch2*$^{-/-}$ reporter cells
883 transfected with *Gli-Luc* and *Ptch1* were co-cultured with mock, *Shh*, *ShhC25S*, *ShhN*, *ShhN-C25S*,
884 *Shh-C199A*, *Shh:CD4*, or *Shh:GFP* transfected *Ptch1*$^{LacZ/LacZ}$;*Ptch2*$^{-/-}$ cells. Luciferase levels in
885 *Ptch1*$^{LacZ/LacZ}$;*Ptch2*$^{-/-}$ reporter cells co-cultured with Mock transfected cells were set at "1". (C)
886 *Ptch1*$^{LacZ/LacZ}$;*Ptch2*$^{-/-}$ cells were Mock transfected or transfected with *Shh*, *Shh-C25S*, *ShhN*, *ShhN-*
887 *C25S*, *Shh-C199A*, *Shh:CD4*, or *Shh:GFP.* Luciferase levels in Mock transfected *Ptch1*$^{LacZ/LacZ}$;*Ptch2*$^{-}$
888 $^{/-}$ cells were set at "1". (D) *Ptch1*$^{LacZ/LacZ}$;*Ptch2*$^{-/-}$ cells were transfected with *Shh* and *Smo-myc*. Cells
889 were stained for Shh (5E1) (green) and myc (magenta). (E) *Ptch1*$^{LacZ/LacZ}$;*Ptch2*$^{-/-}$cell transfected with
890 *ShhN* and *Smo-myc*. Cells were stained for ShhN (5E1)(green) and myc (magenta). Scale bar is
891 20μm. All error bars are s.e.m., *p* values (Student T-test, 2 tailed) are indicated were relevant, (B) n
892 ≥9, (C) n≥8, all independent biological replicates.

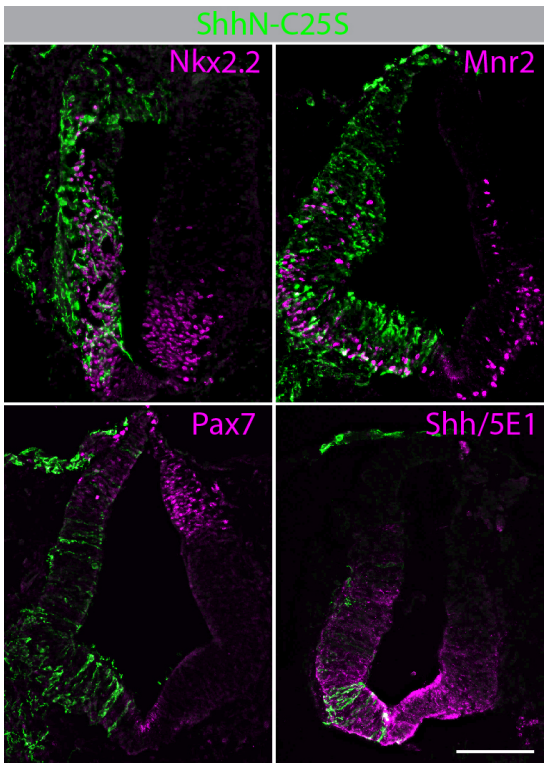

Figure 6, Figure Supplement 1. ShhN-C25S activates the Hh response pathway in vivo

Cross-sections of stage 20 HH chicken neural tubes co-electroporated with *GFP* and *ShhN-C25S* labeled in green. Sections were stained with antibodies to Nkx2.2, Mnr2, Pax7, and Shh (5E1) labeled in magenta. Scale bar is 100μm.

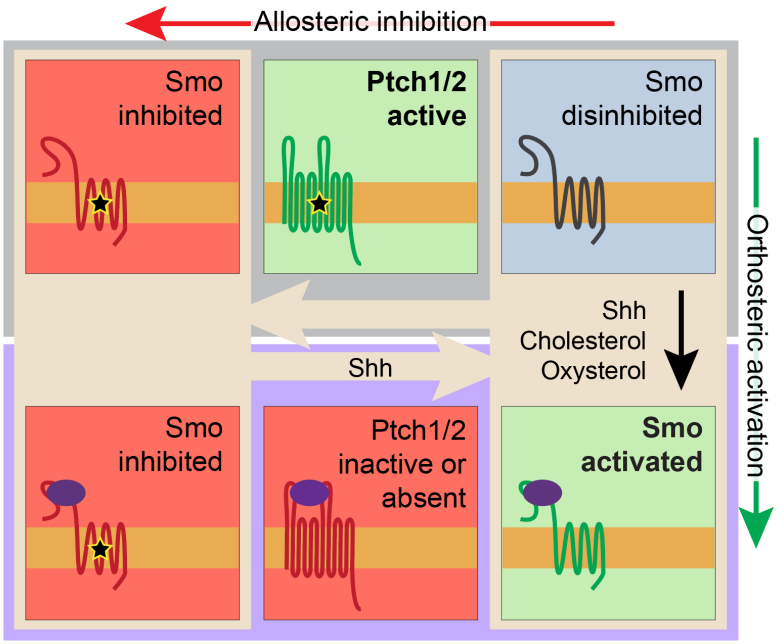

Figure 7. Model

The absence of Shh ligand from the extracellular environment permits the Ptch1/2-mediated allosteric modulation of Smo activity Ptch1/2 (red arrow) through the transportation of an inhibitor (yellow lined black asterisk) that binds to the heptahelical site on Smo. Shh ligand (purple) in the a Ptch1/2 containing receptor complex on the cell membrane via the Shh binding (L2) domain (blue pictogram), causing the inhibition of Smo to be repressed. This allows the accumulation of disinhibited, inactive Smo (top right). This form of Smo is sensitive to (indirect), orthosteric activation by Shh in a Ptch1/2-independent manner (green arrow).